Quantitative Assessment of Dimer Formation by Hypoxia Inducible Transcription Factor Subunits HIF-1α and HIF-2α

Dissertation

presented by

Diplom-Chemist

Jun Hu

from Shanghai, China

in Partial Fulfillment of the Requirements

for the Degree of

Dr. rer. nat.

Faculty of Chemistry

University Duisburg-Essen

July 2013

The present work was performed from February 2010 to July 2013 in the research group of Prof. Dr. Joachim Fandrey at the Institute of Physiology, University Duisburg-Essen, as a graduate student supported by the GRK 1431.

Date of Disputation: 28.01.2014

Supervisor:	Prof. Dr. Joachim Fandrey
	Prof. Dr. Carsten Schmuck
Chairman:	Prof. Dr. Torsten C. Schmidt

Contents

1. Summary

Oxygen homeostasis in cells and tissues is tightly controlled by the transcription factors Hypoxia Inducible Factors (HIFs) which regulate the expression of genes that facilitate O_2 delivery and metabolic adaptation to O_2 deprivation in all mammalian cells (Semenza, 2001). Therefore, HIFs ensure the cells' survival by playing a dominant role in response to ischemia, anemia or systemic hypoxia (Berchner-Pfannschmidt *et al*., 2008). Three isoforms of HIF-α subunits HIF-1α, HIF-2α and HIF-3α differ by their specific sources; however they share highly similar structures (Gu *et al*., 1998). Because of the frequent presence of HIF-1α and HIF-2α, as well the less well understood role of HIF-3α (Loboda *et al*., 2010), the focus of this study was HIF-1α and HIF-2α. Controlling the expression of several hundreds of HIF target genes involved in O_2 transport (erythropoietin), angiogenesis, glucose metabolism, proliferation and survival (Rankin *et al*., 2008), HIF-1α and HIF-2α were intensively studied in recent years. However, neither the physiology nor the pathophysiology is fully resolved as "master regulators of oxygen homeostasis" (Semenza, 1998). To obtain better understanding of the HIFs' regulation, confocal microscopic fluorescence resonance energy transfer (FRET) was applied for investigating the protein-protein interaction between the subunits. In order to show the function of basic helix-loop-helix (bHLH) and Period/Arnt/Single-minded (PAS) domains, deletion and single nucleotide mutations were performed on HIF-1α and HIF-2α. It is evident that a basis to explain some of the target gene specificity observed with HIF-1 versus HIF-2 driven genes can be provided by the new findings in this study.

2. Introduction

2.1 Structure of Hypoxia Inducible Factors (HIFs)

HIF is expressed ubiquitously as a heterodimer (Semenza, 1996) consisting of α- (human HIF-1α: 826 amino acids, 120 kD; human HIF-2α: 870 amino acids, 118 kD; Lau *et al*., 2007) and the β-subunit (human HIF-1β: 774-789 amino acids, 91-94 kD) also known as aryl hydrocarbon nuclear translocator (ARNT; Wang *et al*., 1995). All subunits belong to the bHLH (basic helix-loop-helix) PAS (Period/Arnt/Single-minded) transcription factor family (Wang *et al*., 1995). These two N-terminal located bHLH- and PAS-domains are essential for the formation of α/β heterodimers and sequence-specific DNA binding (Gu *et al*., 2000). The following ODD domain (oxygen-dependent degradation domain) and the N-TAD domain (N-terminal transactivation domain), only present in α-subunits (Fig. 2-1), are recognized by PHD 1-3 (prolyl hydroxylase-domains 1-3) for O_2-dependent hydroxylation and targeting for subsequent degradation by the proteasomes (Fandrey *et al*., 2006). The lack of the ODD and N-TAD in ARNT causes its constitutive expression in the cell nucleus. The C-TAD domain (C-terminal transactivation domain), acts to recruit transcriptional co-regulatory proteins like p300/CBP and is shared both in α-subunits (Fig. 2-1; Fandrey *et al*., 2009). These structural characteristics are shared to a high degree by the HIF-1α and HIF-2α isoforms: 85 % in the bHLH domain, 70 % in the PAS domain, 69 % in the ODD domain, 70 % in the N-TAD domain and 69 % in the C-TAD domain are identical (Hu *et al*., 2007).

In this study, the function of bHLH and PAS domains were determined. The bHLH domain, consisting of 60 amino acids, is composed of an N-terminal basic region functioning for DNA binding, and a C-terminal HLH region involve in dimerization (Murre *et al*., 1994; Fig. 2-2 A). The interaction between the HLH regions of two separate polypeptides leads to the formation of

homodimers and/or heterodimers and subsequent specific DNA-sequence recognition (Carretero-Paulet *et al*., 2010). The following PAS domain is widespread as signal transduction proteins, currently identified in 2000 proteins from organisms in all three kingdoms of life and is further subdivided into a PAS A- (N-terminal) and a PAS B- (more C-terminal) domain within the entire PAS stretch (Möglich *et al*., 2009). Usually, PAS consists of about 120 amino acids. A five-stranded antiparallel β-sheet structure was determined to be required for hetero- and homodimerization (Card *et al*., 2005; Fig. 2-2 B).

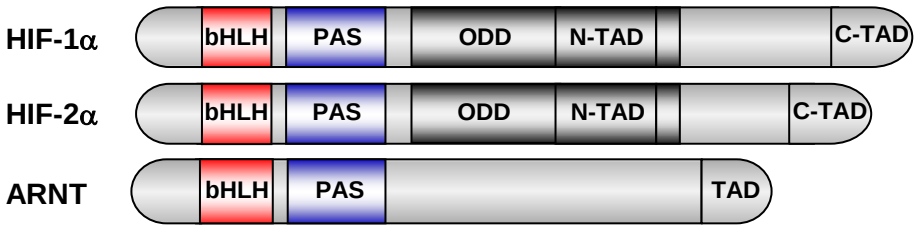

Fig. 2-1: Structure of hypoxia inducible factors

HIF-1α, HIF-2α and ARNT locate in human gene chromosome 14, 2, and 1, respectively (Szablowska-Gadomska *et al*., 2011). bHLH and PAS domains are responsible for DNA binding and dimerization. ODD and N-TAD domains, present only in α-subunits, serve as targets for hydroxylation at their proline residues. C-TAD possesses a p300/CBP binding site for the transactivation.

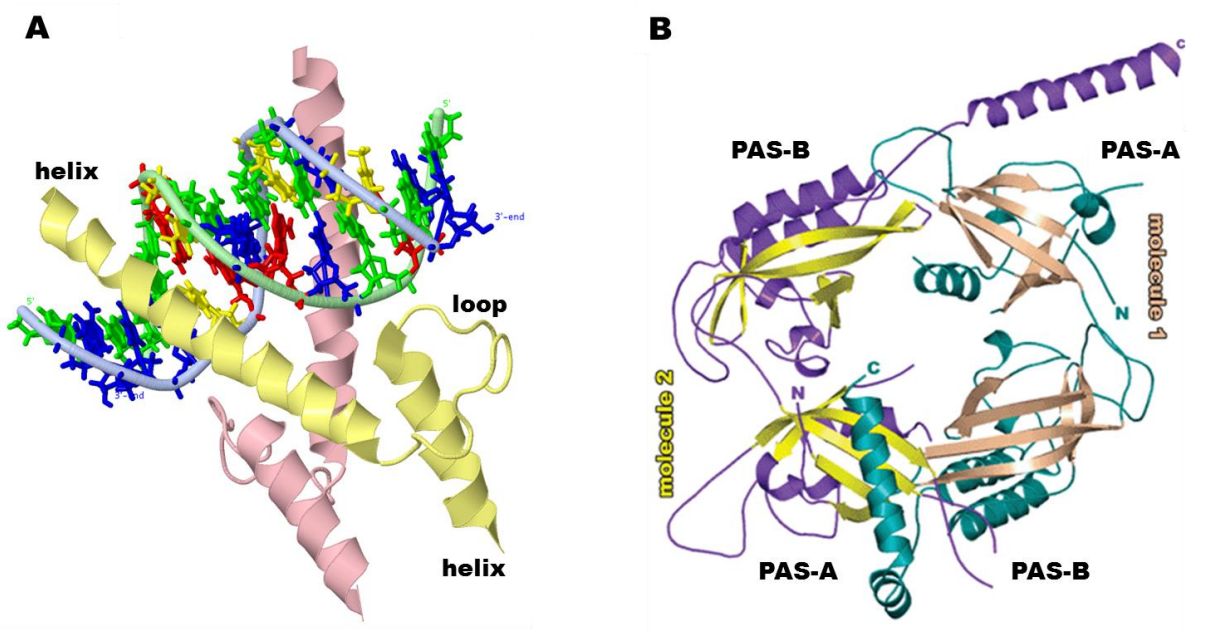

Fig. 2-2: Structure of bHLH (A) and PAS (B)

(A) Structural, bHLH domain is responsible for DNA-binding (N-terminal basic region) and dimerization (C-terminal HLH region; modified from Michel *et al.*, 2000). (B) PAS, contributing for dimerization, consists of PAS-A and PAS-B domains with anti-parallel structure, provided by two molecules (modified from Chowdhury *et al.*, 2008).

2.2 Oxygen Dependent Activation of HIF

In normoxic condition, both HIF-1α and HIF-2α subunits are rapidly post-translationally hydroxylated at proline residues (HIF-1α: P402 and P564, HIF-2α: P405 and P531) by oxygen sensitive enzymes with prolyl hydroxylase-domains (PHD 1, 2 and 3; Jaakkola *et al.*, 2001, Ivan *et al.*, 2001 and Bruick, McKnight, 2001). The activity of PHDs is dependent on oxygen, therefore the PHDs are called cellular oxygen sensor (Berchner-Pfannschmidt *et al.*, 2008). Moreover, the co-substrate 2-oxoglutarate, iron (II) cofactors and vitamin C are required for the hydroxylation of HIF-α subunits (Nytko *et al.*, 2011). Hydroxylated HIF-αs are recognized by the von-Hippel-Lindau protein, rapidly polyubiquitinylated and degraded by 26S proteasome (Schofield *et al.*, 2005 and Fandrey *et al.*, 2006). Thus, HIF-αs are undetectable in most cells under well oxygenated conditions; however in hypoxia, PHD activity ceases (Berchner-

Pfannschmidt *et al*., 2007), which makes the hydroxylation infeasible, so that the stabilized HIF-α subunits accumulate and translocate into nuclear through their NLS (nuclear localization sequence) at the N-terminal end of α-subunits. Then, HIF-α subunits dimerize with the constitutively expressed ARNT subunit in the nucleus. The interaction takes place via the bHLH and PAS domains and a functional DNA-binding complex is formed. This then specifically binds the well conserved HIF binding site (HBS) within hypoxia response elements (HRE) 5'-NCGTG-3' (wherein N is either A or G) and leads to transcription of the corresponding target genes, such as carbonic anhydrase 9 (CA9), vascular endothelial growth factor (VEGF), adrenomedullin (ADM) and erythropoietin (EPO; Semenza, 2001). In addition to the degradation of the α-subunit under normoxia, the transcriptional activity of HIF can be blocked by hydroxylation of an asparagine residue in the C-terminal transactivation domain (C-TAD), since the recruitment of transcriptional cofactor p300/CBP (cAMP response element binding protein) is prevented by asparagine hydroxylase called factor inhibiting HIF-1 (FIH-1; Fandrey *et al*., 2006).

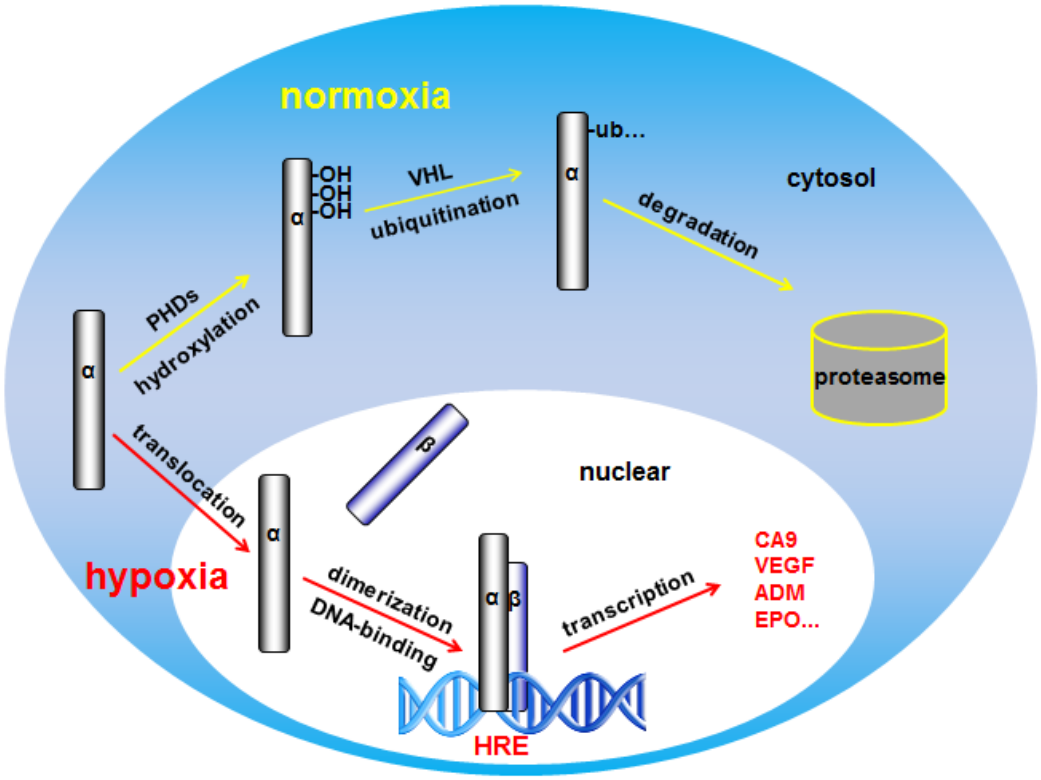

Fig. 2-3: HIF-α mediated pathway of O_2 sensing

HIF-αs accumulate in hypoxia (pathway with red arrows) and translocate into nuclear to dimerize with ARNT. Heterocomplexes bind to hypoxia response elements (HRE) of DNA to induce HIF target genes. In normoxia (pathway with yellow arrows), α-subunits are rapidly hydroxylated, ubiquitinylated and degraded in the proteasome.

2.3 HIF-1α and HIF-2α

The structural similarity of the two isoforms HIF-1α and HIF-2α was shown in Fig. 2-1. However, they differ by their cellular localization, oxygen dependent degradation, transcriptional coactivation, a variety of target genes and even the pathological functions (Ratcliffe, 2007). HIF-1α is ubiquitously expressed in all cells whereas HIF-2α is limited to endothelium, kidney, lung, heart and small intestine (Gordan *et al*., 2007). From the first discovery of HIF-1α by Semenza in 1996, over hundreds of HIF-1α target genes have been already identified, whereas the selective HIF-2α responsive genes were only found recently (Covello *et al*., 2006 and Raval *et al*., 2005). Some target genes like VEGF are shared both by HIF-1α and HIF-2α, however, others like EPO is preferentially

regulated by HIF-2α in kidney and liver (Rankin *et al*., 2007). Furthermore, the proapoptotic gene BCL2/adenovirus E1B-interacting protein 1, (NIP3/Bnip3) and a series of gene encoding enzymes involved in the glycolytic pathway as PGK (phosphoglycerate kinase) are characterized as preferential HIF-1α targets (Hu *et al*., 2003; Raval *et al*., 2005). The distinct, tissue specific target genes raise the question about how the HIF-1α and HIF-2α are working together in hypoxia. The knockout of both subunits is lethal (Huang and Bunn, 2003). Moreover, HIF-2α affects the vascular function and angiogenesis in vascular endothelial cells (Skuli *et al*., 2009), promotes growth and metastasis in neuroblastomas (Holmquist-Mengelbier *et al*., 2006). HIF-2α is involved in the genesis of renal carcinoma with the von Hippel-Lindau syndrome (Kondo *et al*., 2003), however it inhibited the growth of breast cells (Blancher *et al*., 2000), in which the HIF-1α is required for induction with a set of well-characterized hypoxic genes (Sowter *et al*., 2003). Recent data of Yuan *et al*. provided evidence that the mutual antagonism between HIF-1α and HIF-2α may be through the regulation of ROS (reactive oxygen species; Yuan *et al*., 2012). All these facets make the understanding of the molecular regulation of HIF-1α and HIF-2α eminently important.

2.4 Aim of the Study

In this study, we examined hetero- and homodimerization of HIF-subunits using fluorescence resonance energy transfer (FRET). To understand the molecular function of bHLH and PAS domains, deletions and single nucleotide mutations were performed. Labeling of HIF subunits with cyano fluorescent protein (CFP) and yellow fluorescent protein (YFP) allowed the identification in the microscopic study and provided the basis for FRET (Fig. 2-4). In addition, co-immunoprecipitation was performed to confirm the FRET results. Electro-Mobility-Shift-Assays (EMSA) were carried out to test for potential DNA-

binding of homodimers and the activity was determined by activation of a HIF-1 driven luciferase reporter gene and quantitation of target gene expression.

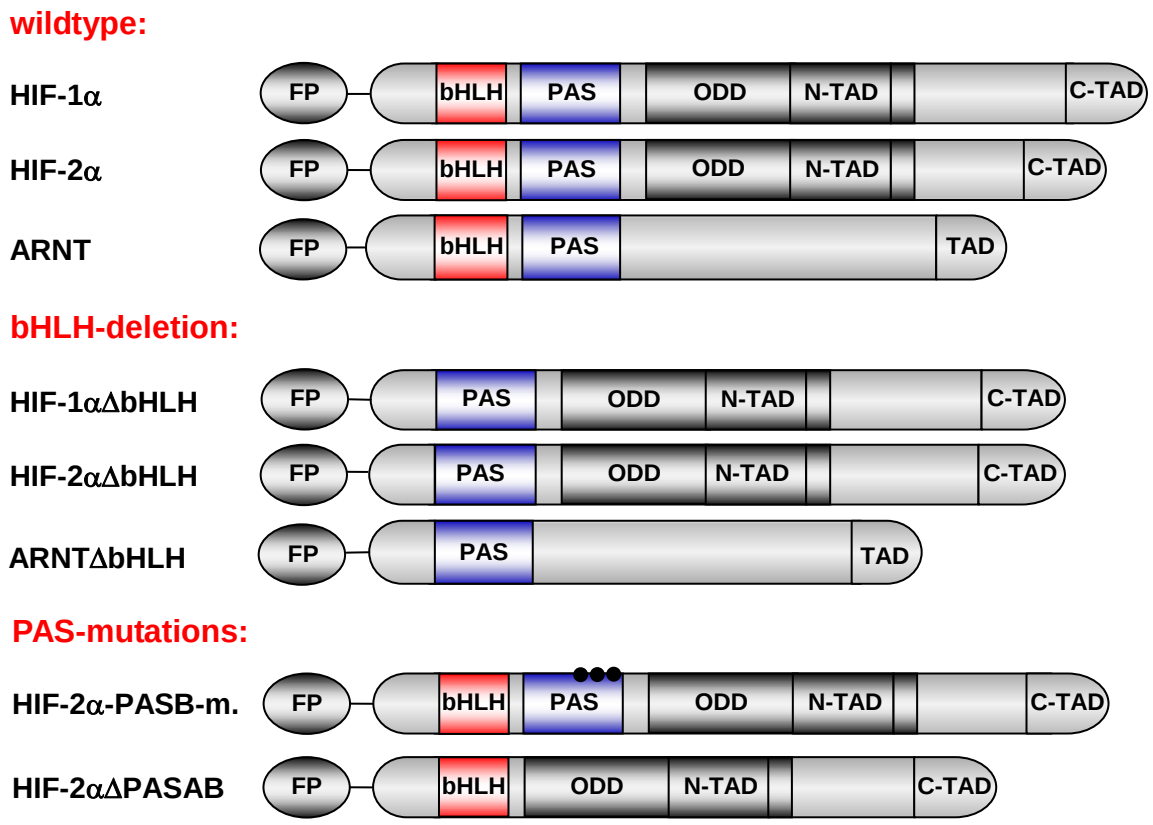

Fig. 2-4: Fluorescent protein-HIF fusion protein constructs used in this study

Wildtype (the top section), bHLH-deleted (the middle section) and PAS-mutant (triple dots mutation and PASAB-deletion, the bottom section) HIF-subunits were generated and applied. For FRET study, all constructures were labeled with fluorescence proteins (CFP or YFP). Constructs in detail see table 3-17.

3. Materials and Methods

3.1 Cell Culture of the Eukaryotic Cells

The cell line U2OS (osteosarcoma, ATCC No. HTB-96) was used for the whole study. U2OS were grown as monolayer in the cell culture with medium DMEM (Dulbecco's Modified Eagle's Medium, Gibco) with 10 % FCS, 100 U/ml penicillin and 100 U/ml Streptomycin sulfate (Gibco). Cells were incubated in 75 cm^2 culture flask with 5 % CO_2 in air and 100 % humidity in 37 ℃ incubator. The medium was replaced every 3 days.

Fig. 3-1: Schema of cell flask and medium

Cells were cultured in flask (Cellstar®) with 15 ml medium (DMEM, Gibco).

3.2 Protein-Biological Methods

Generation of Cell Lysates

0.2-0.8×10^5, 1-3×10^5, 1-3×10^5 and 5-10×10^5 cells were plated on 24-well plates (for luciferase reporter gene assay), 6-well plates (for Western blot), 35 mm

diameter dishes (for FRET) and 60 mm dishes (for Electro-Mobility-Shift-Assay and co-immunoprecipitation) respectively (50-60 % cellular confluence) and incubated for 1 day for further experiments. To generate the cell lysate, cell culture medium was removed and all plates and dishes were rinsed with cold PBS buffer placed on ice. Immediately, 50 µl lysis buffer (50 µl Igepal (0.1 % NP40), 30 ml 0.5 M sodium chloride, 500 µl 1 M Tris pH 7.9, 100 µl 0.5 M EDTA, 18.9 ml 1×PBS) with 10 % protein inhibitor was added to the cells for Western blot analysis and 500 µl lysis buffer (1 % NP40, 0.15 M sodium chloride, 2 mM EDTA, 10 mM sodium phosphate, pH 7.2) with 10 % protein inhibitor was added to the cells for co-immunoprecipitation. Using a cell scraper, the cells were removed from the bottom of the dishes and transferred to an 1.5 ml Eppendorf tube. After incubation on ice for 20 min, supernatant was separated from the cell debris through centrifugation at 3600 rpm at 4 ℃ for 5 min. 5 µl supernatant was needed for protein determination and the rest was stored at -20 ℃ for further study.

Protein Determination

Protein concentration was determined in whole cell lysates with the Dc protein assay kit (BioRad). The prepared 5 µl lysate was diluted with deionized water to a final volume of 50 µl. 20 µl was pipetted onto a 96 well plate for protein determination in duplicate. To each well, 10 µl reagent A (containing sodium carbonate, sodium bicarbonate, bicinchoninic acid and sodium tartrate in 0.1 M sodium hydroxide) and 75 µl reagent B (containing 4 % cupric sulfate) were added. Simultaneously, standard series of albumin (25, 10, 5, 2.5, 1, 0.5, 0.25 and 0.1 mg/ml) and a water sample were treated in the same way. After 5 min incubation at room temperature, a blue color developed and the absorbance was measured at 700 nm in the plate reader Epoch (BioTek) using the albumin as a standard.

SDS-PAGE and Western Blot

Proteins were separated by SDS-PAGE under denaturing conditions according to Laemmli (1970). The samples were added to 4×SDS-sample buffer (0.4 ml *a.dest.*, 1.6 ml 0.5 M Tris pH 6.8, 1.6 ml glycerin, 3.2 ml 10 % SDS, 0.8 ml β-mercaptoethanol, 0.4 ml 0.5 % (w / v) bromphenolblau). Under heat conditions (5 min. at 95 °C), the proteins were denatured with SDS (*sodium dodecyl sulfate*). The poly acrylamide gel was composed of 5 % collecting gel (2.9 ml *a.dest.*, 0.83 ml acrylamide/bisacrylamide, 1.25 ml 0.5 M Tris pH 6.8, 50 µl 10 % SDS, 25 µl 10 % APS, 5 µl TEMED) and 7.5 % (4.9 ml *a.dest.*, 2.5 ml acrylamide/bisacrylamide, 2.5 ml 1.5 M Tris pH 8.8, 100 µl 10 % SDS, 50 µl 10 % APS, 5 µl TEMED) separating gel. The buffer was made up as follows: 0.5 M Tris pH 6.8: 91 g Tris was solved in 400 ml *a.dest.*. The pH value was adjusted with 32 % HCl to 6.8 and the total volume was adjusted with *a.dest.* to 500 ml. 1.5 M Tris pH 8.8: 30.3 g Tris was solved in 400 ml *a.dest.*. The pH value was adjusted with 32 % HCl to 8.8 and the total volume was adjusted with *a.dest.* to 500 ml. A molecular mass standard marker (Spectra™ Multicolor Broad Range Protein Ladder, Fermentas) was run on the gel with the samples to separate them according to their apparent molecular mass during their movement through the gel in direction of the anode. Gels were run for 90 min at 120 V. Then the samples were blotted onto a nitrocellulose membrane in a Tank-Blot system (BioRad) with 1× blotting buffer (5 g Tris, 72 g glycine, 1 l methanol, *a.dest.* to 5 l) for 90 min at 120 V at 4 °C. With Ponceau S-staining solution (Sigma), blots were checked for the successful and equal transfer. The membrane was washed with TBS-T buffer (50 ml 10×TBS-buffer, 250 µl Tween 20 (Sigma), *a.dest.* to 500 ml). The 10×TBS-buffer was made from 121 g Tris and 400 g sodium chloride. The pH value was adjusted with 32 % HCL to 7.6 and the total volume was adjusted with *a.dest.* to 5 l.

For the specific detection of proteins, the membrane was incubated in 5 % skimmed milk (skimmed milk powder solved in TBS-T) with the primary

antibodies (table 3-1) overnight. After 3 times washing with TBS-T, the corresponding secondary antibodies (solved in 5 % skimmed milk) were added.

Table 3-1 Antibodies for Western blot analysis

antibodies	Description	produced in	dilution	Manufacturers
anti-rabbit	HRP-conjugated	goat	1:10000	Sigma-Aldrich
anti-mouse	HRP-conjugated	goat	1:10000	Sigma-Aldrich
anti-α-tubulin	Monoclonal	mouse	1:1000	Santa Cruz Biotechnology
anti-HIF-1α	Monoclonal	mouse	1:1000	BD Transduction Laboratories
anti-HIF-2α	Polyclonal	rabbit	1:1000	Novus Biologicals
anti-HIF-2α	Polyclonal	rabbit	1:1000	Thermo Scientific
anti-ARNT	Polyclonal	rabbit	1:1000	Cell Signaling
anti-GFP	Polyclonal	rabbit	1:200	Clontech
anti-HA	Polyclonal	rabbit	1:1000	Sigma-Aldrich
anti-GAL4	Monoclonal	mouse	1:1000	Santa Cruz Biotechnology

The detection was performed using the ECL system (Amersham ECL Advance Western-Blotting Detection Kit, GE Healthcare). After 1 h incubation of the membrane with respective secondary antibodies directed against the primary antibodies, membranes were washed 3 times and then incubated with each 250 µl reagent A and B from the ECL-kits. Luminescent light was collected with a Fusion (PEQLAB Biotechnologie) system and documented for further evaluation.

Co-Immunoprecipitation

For the co-immunoprecipitation experiment, GAL4-HIF-2α HA-HIF-1α and HA-HIF-2α (Prof. E Metzen, Essen, Germany) were used. Procedures were performed at 4 ℃. Cells were added to NP40 lysis buffer. Protein concentration was measured and 500 µg proteins were transferred into 1.5 ml Eppendorf tube. Total volume was adjusted with lysis buffer to 500 µl. Protein was incubated with 4 µl agarose conjugated anti-GAL4 antibody (500 µg/0.25 ml, Santa Cruz

Biotechnology) and rotated overnight, so that the protein with GAL4-tag was immunoprecipitated. Next day, the agarose binding pellet was spun down and washed 5 times with each 1 ml NP40 lysis buffer to remove the unbound proteins. Finally, the pellet was resuspended with 10 µl 4×SDS, boiled for 5 min at 95 °C with vortexing every 30 s to release the agarose and loaded onto the Western blot gel. Anti-HA antibodies (Sigma-Aldrich) were used to detect the co-immunoprecipitated protein with HA-tag.

Electro-Mobility-Shift-Assay

Double-stranded asymmetric W18 (AGCTTGCCCTA**CGTG**CTGTCTCAG) and palindrome hBnip3 oligonucleotides (ACGCGCCGCA**CGTG**CCACACGCAC) including the HRE (bold letters) of the erythropoietin gene were annealed and labeled with radioactive ^{32}P with T4 DNA polynucleotide kinase. Nuclear extracts generated by NE-PER Nuclear and Cytoplasmic Extraction Kit (Thermo Scientific) were dialyzed with 4×dialysis buffer (1 mM sodium orthovanadate, 0.5 mM dithiothreitol (DTT), 20 mM Tris-HCL and 100 mM KCL were dissolved in 1500 ml *a.dest*., 20 % glycerol and 0.5 M EDTA were added. The pH was adjusted to 7.8 with 37 % HCL and total volume was made up to 2 l with *a.dest*.) and subsequently incubated with 4×dialysis buffer, 5×binding buffer (25 mM Tris-HCL, 125 mM KCL, 5 mM $MgCl_2$, 4.75 mM EDTA, 25 mM DTT, 0.15 % NP40), PolydI-dC(150 ng/ul), mutant sample (1000 ng/µl), sterile water, competitor (unlabeled oligonucleotide) and antibody (in case of supershift) for 5 min at room temperature. The ^{32}P-labelled oligo probe was added and incubated at room temperature for another 20 min. Prerun of the 5 % native polyacrylamide gel was done at 300 V and 4 °C for about 30 min and then the samples were loaded on the gel. The gel was run in 0.5×Tris-Borate EDTA buffer (5×TBE: 54 g Tris base, 27.5 g boric acid and 0.5 M EDTA (pH 8.0) were solved in *a.dest.* up to 1 l with pH 8.0) at 300 V in the cold room (at 4 °C) for about 45 min. The gel was

dried in vacuum at 85 ℃ for 2 h. Finally, the samples were transferred to the plastic wrap, which could be exposed and developed under X-ray.

3.3 RNA Methods

Isolation of RNA from Cells

Cells were cultured in 6 well plates to a confluence of 50-60 % for respective experiments. All experiments were performed in triplicate. To isolate the RNA, culture medium was drawn off on ice, 700 µl 4 M GTC (236.4 g guanidium thiocyanate, 4.18 ml 3 M NaOAc, pH 5.2, in 500 ml DEPC-H_2O (500 µl diethylpyrocarbonate (DEPC) in 500 ml *a.dest.*, autoclaved for 40 min) with 3.75 ml β-mercaptoethanol) was added and the samples were stored at -20 ℃ overnight. At the next day, samples were transferred to 2 ml tubes and 70 µl NaAc (16.41 g sodium acetate was solved in 100 ml *a.dest*., to pH 4.0 adjusted with glacial acetic acid) was added. 500 µl phenol (AppliChem) and 350 µl phenol-chloroform-isoamyl (AppliChem) were added under the fume hood. After vortexing, the samples were milky. After storage on ice for 1 h, samples were centrifuged at 13000 rpm for 30 min. The supernatants (only including RNA) were transferred to new 1.5 ml tubes. 500 µl isopropanol (CARLO ERBR) was added and after vortexing, the samples were stored at -20 ℃ overnight. At next day, samples were centrifuged at 13000 rpm and 4 ℃ for another 20 min. The supernatants were carefully removed under the fume hood. The pellets were dried by inverting the tubes on paper towels. Subsequently, 500 µl GTC and 500 µl isopropanol were added to the samples. After vortex, the samples were stored at -20 ℃ overnight. At the next day, the sapmles were centrifuged at 13000 rpm and 4 ℃ for 30 min. After that, the supernatants were carefully removed and samples were dried by inverting the tubes on paper towels. 500 µl 75 % ethanol (100 % ethanol diluted in DEPC-H_2O) was added to the samples and the samples were incubated at room temperature for 30 min. After short vortexing, the samples were centrifuged at 13000 rpm and 4 ℃ for

30 min. The supernatants were carefully removed and the pellets were dried at room temperature for about 45 min to ensure the complete removal of the solvent. From this step stuffed pipette tips had to be used to avoid the degradation of mRNA. The samples were dissolved in 10-20 µl DEPC-H_2O at 60 ℃ and 1 µl samples were used for photometric measurement using the Epoch (BioTek) using 260 nm for determination of the RNA concentration and 280 nm for determination of the protein contamination. Usually a ratio for 260/280 nm of 1.8 was achieved. mRNA samples were stored at -80 ℃.

Reverse Transcription

For reverse transcription (RT) of mRNA into single-stranded complementary DNA (cDNA), mRNA was transcribed using oligo-(dT), dNTPs and reverse transcriptase (MMLV-RT, Promega). For the RT, DEPC-H_2O was added to 1 µg mRNA with 2.5 µl oligo-dT to the total volume of 12 µl. Samples were heated at 68 ℃ for 10 min, to denature secondary RNA structures and allow oligo-dT to bind to the poly-A tail of the mRNA. After cooling down of the samples on ice, 13 µl RT-mix (for each sample, 5 µl 5×RT-buffer, 5 µl dNTP, 0.5 µl MMLV-RT and 2.5 µl H_2O) was added to each sample. The transcription was carried out as shown in table 3-2:

Table 3-2 RT-program

cycles	temperature (℃)	time (min)
1×	45	90
1×	52	30
1×	96	15

The cDNAs were shortly stored at 4 ℃ and long-term at -20 ℃.

PCR

With the help of a qualitative PCR (*polymerase chain reaction*), the quality of RT was checked. The GoTaq DNA polymerase was used to amplify the investigated gene. Primers were chosen so that they were also suitable for qRT-PCR (*quantitative real time* PCR) and approximately 100-150 bp in size PCR-products were produced. 24.5 µl of mix (5 µl 5×buffer, 2 µl dNTPs, 0.5 µl primer s, 0.5 µl primer a, 16.5 µl H_2O and 0.05 µl GoTaq polymerase) were mixed with 0.5 µl cDNA from the previous RT. The PCRs for β-actin and carbonic anhydrase 9 (CA9) were carried out as shown in the following tables 3-3 and 3-4.

Table 3-3 PCR-program for β-actin in reverse transcription

cycles	temperature (℃)	Time
1×	96	3 min
25×	96	1 min
	60	90 sec
	72	3 min
1×	72	10 min

Table 3-4 PCR-program for carbonic anhydrase 9 in reverse transcription

cycles	temperature (℃)	Time
1×	96	3 min
30×	96	1 min
	60	90 sec
	72	3 min
1×	72	10 min

The PCR-products were run in agarose gels with 2 % ethidium bromide, which intercalates into DNA to make PCR products fluorescent after UV-light excitation for photo documentation. β-actin served as a housekeeping gene and

was unchanged. The annealing temperature was adjusted according to the gene-specific primers.

Quantitative Real Time-PCR

For the quantitative analysis of cDNA, the real time PCR was performed using the Mesa Green qPCR MasterMix® Plus for SYBR assay (Eurogentec). Gene-specific primers and β-actin primers were used as in the following table:

Table 3-5 Primers for quantification (Invitrogen)

gene	name	sequence 5'→3'
β-actin	hactin 3'	CAG CGG AAC CGC TCA TTG CCA ATG G
	hactin 5'	TCA CCC ACA CTG TGC CCA TCT ACG A
CA9	hCA9 3'	CAG CGA TTT CTT CCA AGC G
	hCA9 5'	CAC GTG GTT CAC CTC AGC AC

Master mix solution for determination in duplicate was mixed with 25 µl 2×MasterMix®, 22 µl H_2O, 1 µl primer 5' and 1 µl primer 3'. 1 µl cDNA was added to 49 µl mix. The PCR-programs were shown in the following table 3-6 and 3-7.

Table 3-6 PCR-program for β-actin in quantitative real time-PCR

cycles	temperature (℃)	Time
1×	95	10 min
35×	95	15 sec
	60	1 min

Table 3-7 PCR-program for carbonic anhydrase 9 in quantitative real time-PCR

cycles	temperature (℃)	time
1×	95	10 min
40×	95	15 sec
	60	1 min

The analysis was carried out using delta-delta ct method with the formula:
2^-ddCT = 2^-((CT-target - CT-endo)-time2 - (CT-target - CT-endo)-time1)

3.4 Molecular-Biological Method

Gateway®-Cloning System

Based on the bacteriophage lambda site-specific recombination system, the Gateway Technology facilitates the integration of lambda phage DNA into the *E. coli* chromosome and the switch between the lytic and lysogenic pathways (Ptashne, 1992). The lysogenic pathway is catalyzed by the bacteriophage λ Integrase (Int) and *E. coli* Integration Host Factor (IHF) proteins (BP Clonase™ II enzyme mix, Invitrogen) while the lytic pathway is catalyzed by the bacteriophage λ Int and Excisionase (Xis) proteins, and the *E. coli* Integration Host Factor protein (LR Clonase™ II enzyme mix, Invitrogen; Landy, 1989; Ptashne, 1992). As in the following table shown, two recombination reactions constitute the basis of the Gateway: BP reaction and LR reaction.

Table 3-8 Recombination reactions of Gateway system

name	reaction	pathway	enzymes
BP	*att*B ×*att*P → *att*L ×*att*R	lysogenic	BP Clonase™
LR	*att*L ×*att*R → *att*B ×*att*P	lytic	LR Clonase™

The BP reaction is carried out with an *att*B substrate (*att*B-PCR product or a linearized *att*B expression clone) and an *att*P substrate (donor vector, in this study pDONR/Zeo) to create a gene of interest included *att*L-entry clone and a by-product *att*R-*ccd*B.

Fig. 3-2: Schema of BP reaction (modified from Invitrogen)

The key point of the Gateway system is the gene of interest involved entry clone, which can be generated form the BP reaction catalyzed by BP Clonase. *att*B sites are flanked to the gene of interest by PCR, so that the gene exchanges the *ccd*B of the donor vector.

The LR reaction is carried out with an *att*L substrate (gene of interest included *att*L-entry clone) and an *att*R substrate (destination vector, in this study pcDNA 6.2-N-CFP/YFP-DEST) to create an *att*B-containing expression clone and a by-product *att*P-*ccd*B.

Fig. 3-3: Schema of LR reaction (modified from Invitrogen)

To generate an expression clone with the gene of interest, the *att*L flanked entry clone reacts with the *att*R flanked destination vector catalyzed with LR Clonase.

BP Reaction

In this study, N-terminal fused pExp-CFP-HIF-2αΔPASAB and pExp-CFP-HIF-2αPASBm. were cloned from native HIF-2αΔPASAB and HIF-2αPASBm. (Yang *et al*., 2005) for the FRET study. For this purpose, *att*B PCR product with the gene of interest was firstly generated from the two native plasmids. To

design the primers, expression elements like ribosome recognition sequences, start codon, stop codons and reading frame were considered (table 3-9).

Table 3-9 Primers involved *att*B to amplify the N-terminal of gene

name	Sequences
*att*B1	**GGGGACAAGTTTGTCAAAAAAGCAGGCT**TC ATGACAGCTGACAAGGAGAAGAAAAGG
*att*B2	ATATATT**GGGGACCACTTTGTACAAGAAAGCTGGGT**C TCAGGTGGCCTGGTCCAG

In tab. 3-9, bold labeled sequences are *att*B sites. Red labeled sequences are start and stop codons. The rest are HIF-2α specific sequences. The PCR reaction was carried out with *PfuTurbo* DNA polymerase (Fermentas) as shown in the following tables:

Table 3-10 PCR-program for *att*B-HIF-2αΔPASAB

cycles	temperature (℃)	time
1×	95	2 min
30×	95	30 sec
	57	30 sec
	72	2 min
1×	72	10 min

Table 3-11 PCR-program for *att*B-HIF-2αPASBm.

cycles	temperature (℃)	time
1×	95	2 min
30×	95	30 sec
	58	30 sec
	72	3 min
1×	72	10 min

150 ng (1-7 µl) PCR products with the *att*B sites were mixed with 1 µl 150 ng/µl donor vector (pDONR/Zeo, see Fig. 3-4) and 8 µl TE buffer pH 8.0. 2 µl BP Clonase was added to the mix and incubated at room temperature overnight. 1 µl Proteinase K was added to each sample and incubated at 37 ℃ for 10 min to terminate the reaction.

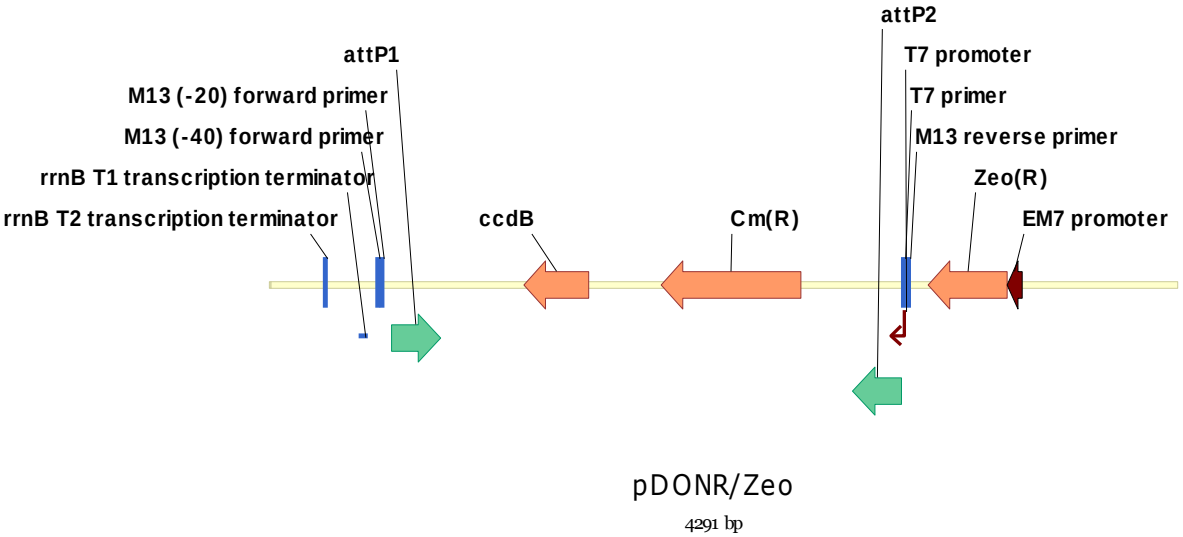

Fig. 3-4: Feature map of pDONR/Zeo (modified from Invitrogen)

Donor vector as pDONR/Zeo is flanked with *att*P sites. *ccd*B gene allows negative selection in *E. coli* like TOP10 and DH5α. Cm (R) (Chloramphenicol resistance gene) is for counterselection. Additionally, pDONR/Zeo is kanamycin resistant.

During the BP reaction, the gene of interest in the *att*B PCR product exchanged the *ccd*B gene of pDONR/Zeo (inhibited to growth in most *E. coli* because of

the interfering with *E. coli* DNA gyrase (Bernard and Couturier, 1992) by the *ccd*B gene) to form the entry clone (Fig. 3-2), which was kanamycin resistant, and a linearized by-product *att*R-*ccd*B. After transformation, selection with kanamycin plate and isolation of DNA, the entry vector was ready for the further LR reaction.

LR Reaction

150 ng kanamycin resistant entry vector from last step (1-7 µl) was mixed with 1 µl 150 ng/µl destination vector (pcDNA 6.2-N-CFP-DEST, see Fig. 3-5) and 8 µl TE buffer pH 8.0. 2 µl LR Clonase was added to the mix and incubated at room temperature overnight. 1 µl Proteinase K was added to each sample and incubated at 37 ℃ for 10 min to terminate the reaction.

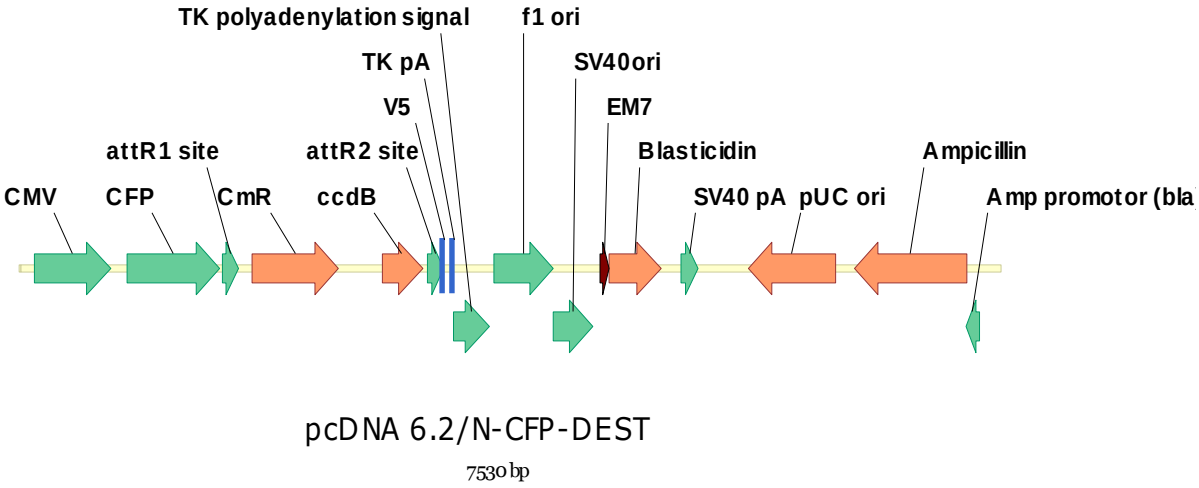

Fig. 3-5: Feature map of pcDNA 6.2-N-CFP-DEST (cloned by Dr. Rebecca Konietzky)
Destination vector as pcDNA 6.2-N-CFP-DEST is flanked with *att*R sites. *ccd*B gene allows negative selection in *E. coli* like TOP10 and DH5α. Cm (R) (Chloramphenicol resistance gene) is for counterselection. Additionally, pcDNA 6.2-N-CFP-DEST is ampicillin resistant.

During the LR reaction, the kanamycin resistant entry vector reacted with the ampicillin resistant pcDNA 6.2-N-CFP-DEST (*ccd*B effect) to form expression clone pExp-CFP-HIF-2αΔPASAB (ampicillin resistant) and pExp-HIF-2αPASBm. (ampicillin resistant), and a *ccd*B involved by-product *att*P-*ccd*B

(Fig. 3-3). After transformation, selection with ampicillin plate and isolation of DNA, the expression vectors pExp-CFP-HIF-2αΔPASAB and pExp-HIF-2αPASBm. were ready for further use in the FRET microscopic study.

Creating a Deletion by Overlap Extension PCR

To delete a desired fragment (black fragment in Fig. 3-6) from existing DNA, primers a and d are designed including restriction points on their 5' sides (or the restriction points are involved in the PCR products of step 1 and step 2) for further digests. Primers b and c are designed so that their 3' ends hybridize to template sequence (red fragment of primer b and green fragment of primer c, Fig. 3-6) on one side of the deletion, and the 5' ends are complementary to another side of the deletion (green fragment of primer b and red fragment of primer c, Fig. 3-6).

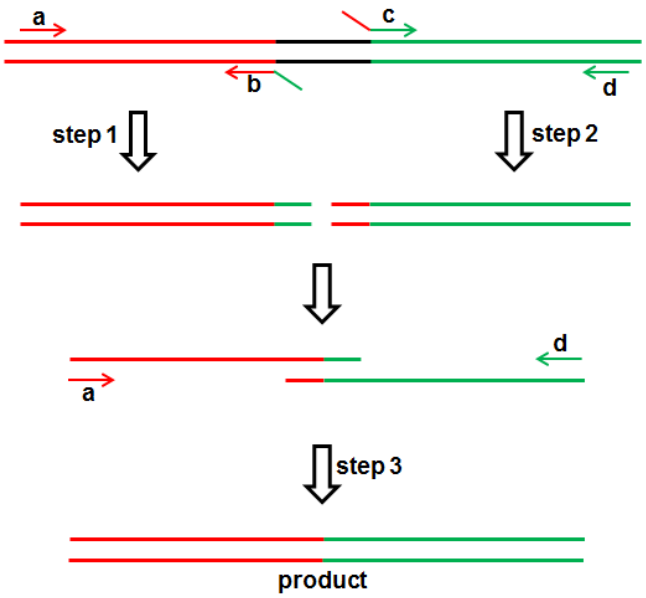

Fig. 3-6: Deletion by overlap extension PCR

The sequence to be deleted is labeled with black lines. The red and green lines indicate the template fragments on either side of the deleted sequence. Primers a, b, c and d are needed for overlap extension PCR. Specially, the primers b and c are designed such that their 5' ends are complementary to template sequence on another side of the deletion.

In this study, the bHLH was deleted form the pExp-YFP-ARNT. According the overlap extension PCR method, primers were designed as in the following table:

Table 3-12 Primers for deletion of bHLH using overlap extension PCR

name	Sequences
ARNTdbHLH-BamHI-s (primer a)	AAGGATCCCTACCGGTGA
ARNTdbHLH-int-a (primer b)	**TGGATGTGTTGCCAGTTCCAAGTCTCTCTTTATCCGCAGA**
ARNTdbHLH-int-s (primer c)	CTCTGCGGATAAAGAGAGACTTGGAACTGGCAACACATCC
ARNTdbHLH-Bsu36I-a (primer d)	TCCTGGAAGACCTCAGGCT

In table 3-12, blue labeled sequences represented the restriction point of primers ARNTdbHLH-BamHI-s and ARNTdbHLH-Bsu36I-a, respectively. The green labeled sequence of primer ARNTdbHLH-int-a was 5' end overhang, which was the complementary end, while the red one bound to the template. The red labeled sequence of primer ARNTdbHLH-int-s was the 5' end overhang, which was the complementary end, while the green one bound to the template. Using these primers, three steps PCRs (Tab. 3-13 to 3-15) were carried out using *PfuTrubo* DNA Polymerase (Fermentas).

Table 3-13 Step 1 of overlap extension PCR-program

cycles	temperature (℃)	Time
1×	95	2 min
30×	95	30 sec
	52	30 sec
	72	1 min 15 sec
1×	72	10 min

Table 3-14 Step 2 of overlap extension PCR-program

cycles	temperature (℃)	Time
1×	95	2 min
30×	95	30 sec
	52	30 sec
	72	2 min
1×	72	10 min

Table 3-15 Step 3 of overlap extension PCR-program

cycles	temperature (℃)	Time
1×	95	2 min
30×	95	30 sec
	54	30 sec
	72	3 min
1×	72	10 min

The bHLH-deleted PCR product from step 3 was double digested with BamHI and Bsu36I (New England BioLabs) and ligated with T4-Ligase (New England BioLabs; see next paragraph) into the original YFP expression vector.

Cleavage of DNA with Restriction Endonuclease and Ligation of DNA Fragments

Phosphodiester bonds of DNA can be hydrolytically split by over 3000 restriction endonucleases specifically (Pingoud *et al*., 2001). The restriction endonucleases differ by source organisms, the recognition sequences and interfaces. The restriction of DNA was carried out in enzyme-specific buffer (NEBuffer 1, 2, 3 and 4, New England BioLabs) at the optimum temperature provided by the manufacturer. In case of double restrictions in one reaction, the software Double Digest Finder from NEB was applied for testing. For the double digest, 1 µg plasmid or PCR product was mixed with 2 µl 10×NEBuffer (1, 2, 3 or 4 according to the enzyme characteristics, New England BioLabs), 2 µl 10×BSA (if necessary, New England BioLabs) and 1 µl enzyme respectively. Total volume was adjusted with H_2O to 20 µl. The mix was incubated at 37 ℃ for 1-2 h.

The ligation of the DNA-fragments was carried out with T4-Ligase (New England BioLabs). Before the ligation, 50 µl insert PCR product was phosphorylated with 1 µl T4 Polynucleotide Kinase (PNK, New England BioLabs), 6 µl 10×PNK buffer and 3 µl H_2O to total volume of 60 µl for 30 min incubation at 37 ℃. The T4 Polynucleotide Kinase was inactivated at 60 ℃ for 20 min. Simultaneously, 50 µl vector needed to be dephosphorylated with 1 µl Antarctic-Phosphatase (New England BioLabs), 6 µl 10×Antarctic-buffer and 3 µl H_2O to total volume of 60 µl for 15 min incubation at 37 ℃. The Antarctic-Phosphatase was inactivated at 65 ℃ for 5 min. Finally, 25 ng dephosphorylated vector was mixed with 5 times phosphorylated PCR insert, 1 µl T4 Ligase, 1 µl 10×ligase buffer to a total volume of 10 µl for 9 h incubation at 16 ℃. 1 µl of the ligated mix was prepared for further transformation.

Transformation

Transformation into bacteria was performed according to the heat shock method described by Sambrook *et al.* (1989). *E. coli* of Top10 (characteristic: F^- *mcr*A Δ (*mrr-hsd*RMS-*mcr*BC) Φ 80*lac* ZΔM15 Δ*lac*X74 *rec*A1 *ara*Δ139 Δ (*ara-Leu*)7697 *gal*U *gal*K *rps*L (Str^R) *end*A1 *nup*G) from Invitrogen was applied. 0.1 µg plasmid was mixed with Top10 *E. coli* and incubated for 30 min on ice. Heat shock was carried out at 42 °C for 30 sec. 250 µl SOC (Invitrogen) was given to the mix and shook for 1 h at 37 °C. After that, 50 µl mix was pipetted to ampicillin (Calbiochem) or kanamycin (Calbiochem) plate (3.5 g Difco Antibiotic Medium 3 (BD Transduction Laboratories), 3 g Select Agar (Life Technologies) were solved with *a.dest.* to total volume of 200 ml and autoclaved. After cooling down, the gel was treated with 200 µl 10 mg/ml antibiotic and allocated to 94 mm dishes with each 20 ml volume) and incubated at 37 °C overnight.

Isolation of Plasmid

The transformed bacteria were incubated in LB medium (10 g trypton, 5 g sodium chloride, 5 g yeast extract (ICN Biomedicals) solved in *a.dest.* to a total volume of 1 l) at 37 °C overnight. The plasmid was isolated using GeneJet Plasmid Miniprep Kit (Fermentas) and PureYield™ Plasmid Midiprep System (Promega) according the guideline of manufacturers.

Determination of Concentration of the Isolated Plasmids

The yield and purity of the plasmid DNA was determined photometrically at wavelengths of 260 and 280 nm using Epoch Take 3 (BioTek).

Sequencing

The sequencing was carried out by Microsynth (Switzerland). The primers for the sequencing are shown in table 3-16.

Table 3-16 Primers for sequencing

name of the vector	sequences
pExp-YFP-ARNTΔbHLH	TACCAGCAGAACACCCCCAT
pENT-HIF-2αPASBm.	TAACGCTAGCATGGATGT
pENT-HIF-2αΔPASAB	TAACGCTAGCATGGATGT

Horizontal Gel Electrophoresis of DNA

The horizontal agarose gel electrophoresis firstly described by Sambrook *et al*. (1989) was used for separation of DNA. Due to the negative charge of phosphate residues, DNA migrated in the electric field to the anode. The linear DNA fragments were separated dependent on their molecular weight. 0.2-2 % (w/v) agarose in Tris acetate-EDTA (TAE)-buffer (50 ×TAE: 242 g Tris, 57.1 ml glacial acetic acid and 100 ml 0.5 M EDTA pH 8.0 were adjusted with *a.dest.* to 1 l total volume) was boiled. The warm solution was treated with 50 µg/ml ethidium bromide solution to reach a concentration of 0.07 % and poured into a gel chamber. Due to its planar properties, ethidium bromide was intercalated into the heteroaromatic rings of the DNA helix. After polymerization, the sample pockets were loaded with size marker (1 kb ladder and 100 bp ladder, New England BioLabs and Invitrogen) and samples. The buffer was filled up to the upper edge of the gels in the chamber and treated with an electric current of 6.25 V/cm. After 2 min pre-running, the chamber was filled with sample buffer to flood the gel. The electrophoresis was carried out at 5 V/cm for 40-60 min. The detection of the DNA was carried out under UV light at an excitation wavelength of 304 nm for ethidium bromide fluorescence.

Purification of DNA Fragments from Agarose Gel

The expected DNA bands with the corresponding sizes were excised from the gel using a scalpel and isolated with QIAquick Gel Extraction Kit (Qiagen) according to the guideline of manufacturer.

3.5 Cytological Methods

Hypoxia Experiment

Since the most HIF target genes like CA9, VEGF and EPO are inducible in hypoxia, cell culture experiments were carried out under hypoxia. For normoxic controls cells were kept in 21 % O_2, 5 % CO_2, 37 °C and 90 % humidity. Culturing the cells in hypoxia was carried out in a hypoxic incubator, equipped with BBL GasPak glasses using BBL™ GasPak™ Plus Anaerobic System Envelopes with Palladium Catalyst (BD BBL). In this study, all the hypoxia experiments were carried out in 1 % hypoxia (1 % O_2, 5 % CO_2, 74 % N_2, and 90 % humidity at 37 °C) for 6 h.

Transient Transfection

The cells were seeded for transfection with a confluence of 50-80 %. Following the guideline of manufacturer, 0.25 µg, 1 µg, 1 µg and 5 µg plasmids and 3 times the amount of GeneJuice® Transfection Reagent (Novagen) were used in 24 well plates (for luciferase reporter gene), 6 well plates (for Western blot), 35 mm dishes (for FRET) and 60 mm dishes (for EMSA and co-immunoprecipitation), respectively. Serum-free medium (20 to 300 µl) was mixed with GeneJuice for 5 min at room temperature. Plasmids were added to this mix and incubated for another 15 min at room temperature. Lastly, the whole mix was directly added to the cells for 24 h incubation and further analysis.

Reporter Gene Assay

For the analysis of HIF activity in U2OS, cells were transfected with a reporter gene (pH3SVL, Fig. 3-7) for the respective experimental conditions (normoxia and hypoxia). The plasmid pH3SVL was provided by Prof. R. Wenger, Zurich (Rolfs *et al*., 1997). The luciferase reporter gene was composed of an SV40

promoter and three HRE (hypoxia-responsive elements) from the 5 'enhancer of the transferrin. The HRE of the transferrin consists of two HBSs (HIF binding sites). During the experiment, luciferase was expressed under control of the HRE and depending on the degree of HIF activation (Fig. 3-7). Using the firefly luciferase assay kit (Biotium), luciferase activity was determined in a luminometer according to the guideline of manufacturer. HIF-activity was expressed relative to total cellular protein concentration. All reporter gene assay experiment was carried as triplicates.

Fig. 3-7: Structure of the pH3SVL

The reporter gene plasmid pH3SVL expressed luciferase under the control of SV40 promoter and three HREs transferrin genes.

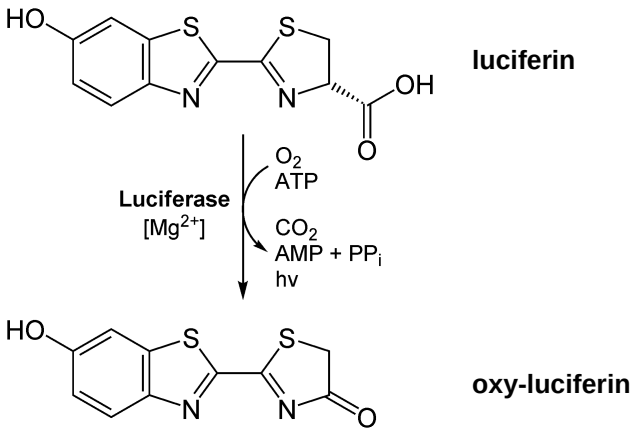

Fig. 3-8: Reaction of the luciferase reporter gene (modified form Yikrazuul)

The luciferin substrate (Biotium) was oxidized by luciferase expressed form pH3SVL to oxy-luciferin releasing with a photon of light as oxyluciferin returned from its exited state to ground state.

3.6 Confocal laser Microscopy

Analysis of Protein-Protein Interactions by FRET

To study protein-protein interactions in living cells, the modern confocal laser microscopy method FRET (fluorescence resonance energy transfer) was applied. This technique depends on the energy transfer between two chromophores, which was firstly described by Theodor Förster in 1926. Usually for FRET, the utilized choromophore pair is CFP (cyan fluorescent protein) and YFP (yellow fluorescent protein). Due to the overlap of the emission spectrum of the CFP and the excitation spectrum of the YFP (Fig. 3-9), energy can be transferred from the excited donor fluorophore (CFP) to the acceptor fluorophore (YFP) through non radiative dipole-dipole coupling, once the donor fluorophore gets close to the acceptor fluorophore. The degree of transferred energy, which is called FRET efficiency, is dependent on the intermolecular protein-protein distance R between the two fluorophores (Fig. 3-10 A). The constant R_0 is named Förster distance, which describes the distance of the fluorophore pair of donor and acceptor, i.e. the distance at which the energy transfer efficiency is 50 % (Fig. 3-10 B). R_0 is flurophore specific and for CFP/YFP pair 4.92 nm (Patterson *et al.*, 2000). Additionally, R_0 was dependent on the refractive index of the donor quantum efficiency, the spectral overlap integral and the relative orientation of the transition dipole moments of donor and acceptor (Lakowicz, 2006)

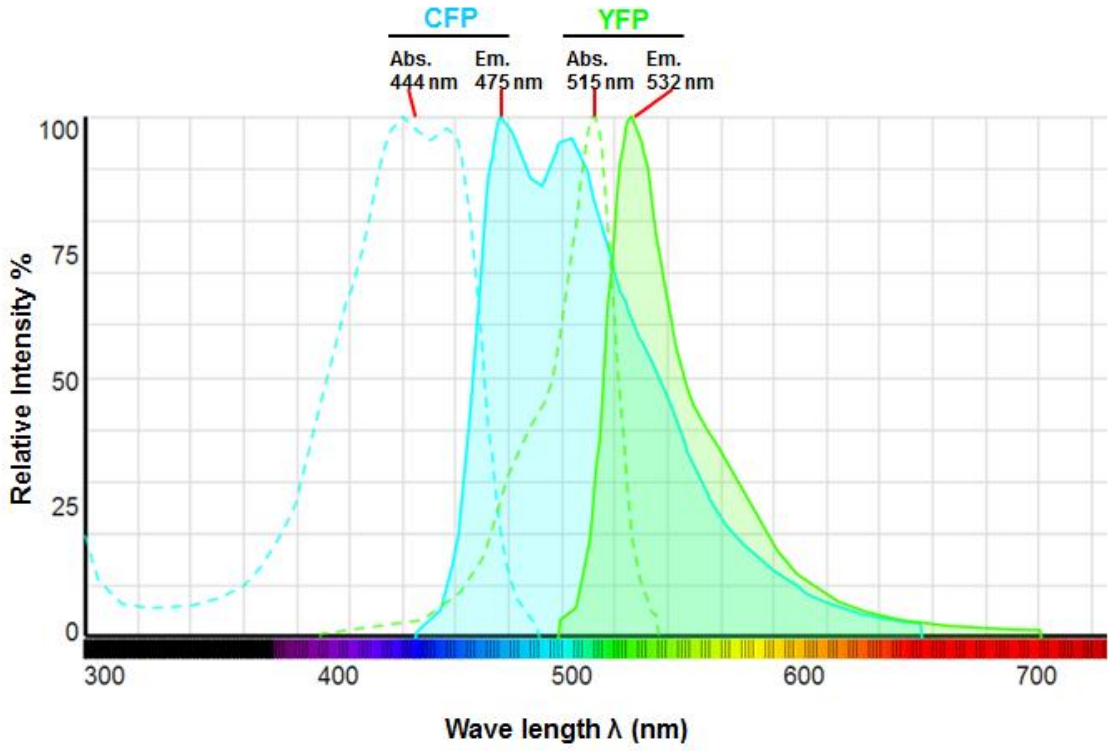

Fig. 3-9: Excitation and emission spectra of CFP and YFP (modified form Fluorescence SpectraViewer of Invitrogen)

The overlapped spectra of emission (CFP) and excitation (YFP) ensure the FRET energy transfer from CFP to YFP.

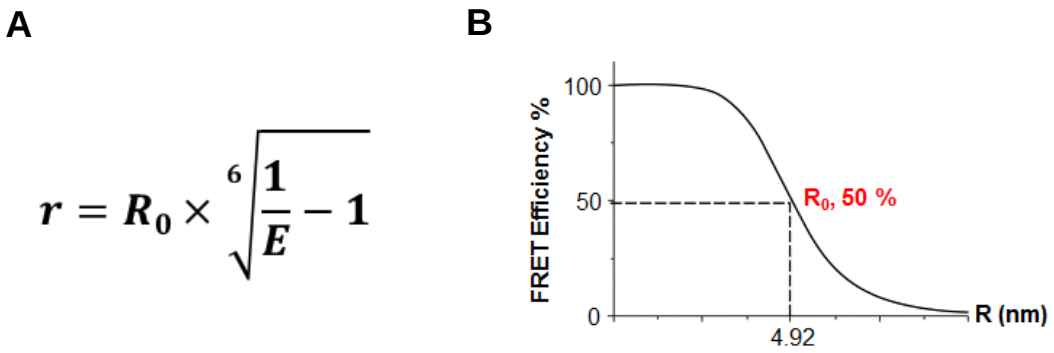

Fig. 3-10: Schema of FRET formula

(A) The distance between two proteins was calculated with the formula, composed of FRET efficiency E and Förster distance R_0. (B) 4.92 nm was the Förster distance R_0 of CFP and YFP, calculated when the FRET efficiency is 50 %.

To apply this method to investigate the protein-protein interaction, all the candidates were labeled with CFP or YFP (Tab. 3-17). Without energy transfer,

the donor (CFP) is excited with the corresponding absorption wavelength (444 nm) and there is a CFP specific emission wavelength at 475 nm (Fig. 3-11). If the distance between the two fusion proteins is less than 10 nm, an energy transfer from CFP to YFP takes place and the emission of CFP is reduced (quenched), since part of the energy is transferred to the acceptor (YFP) to initiate a YFP specific emission wavelength of 532 nm (Fig. 3-11).

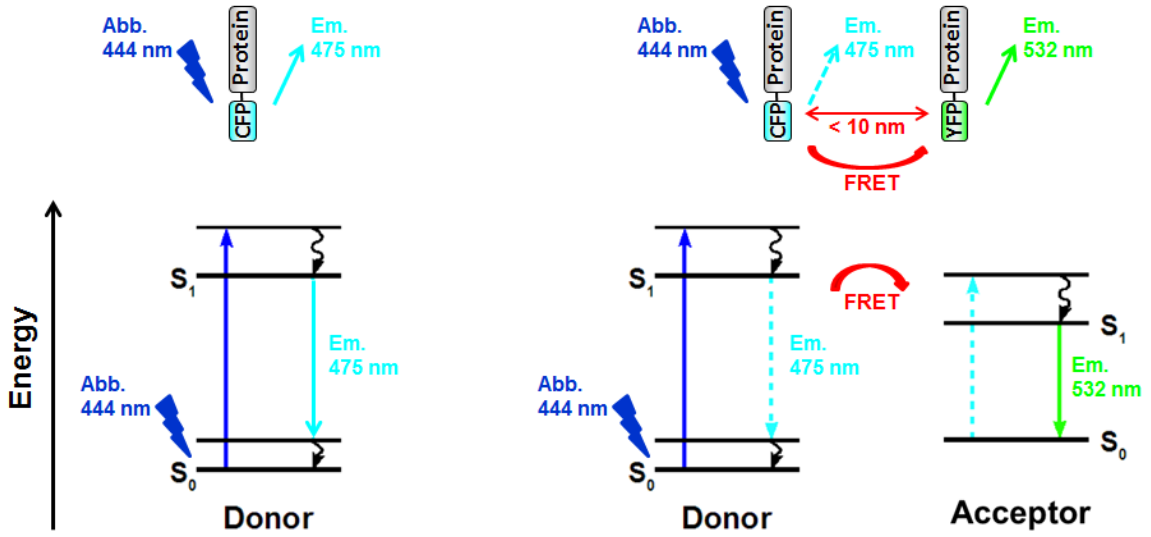

Fig. 3-11: Physical principle of the energy transfer during FRET (modified from S. Jähnichen)

CFP flurophore alone was excited by 444 nm laser and emitted by 475 nm. Physically, the electron was excited from S_0 level to S_1 level and fell back from S_1 to S_0 with an emission of 475 nm. In case the YFP flurophore got close to CFP, the emitted energy of CFP was transferred to YFP non-radiatively so that the YFP was excited and emitted at 532 nm wavelength.

During the experiment, several cells had to be analyzed to get the FRET efficiency, which is recorded against the acceptor/donor (YFP/CFP) ratio. Furthermore, the examination of the final plateau FRET efficiency was calculated using an exponential function (Fig. 4-1). If the plateau of the FRET efficiency was reached, the acceptor/donor ratio did no longer influence the

FRET efficiency. Using the formula (Fig. 3-10 A), the distance between the two partners can be calculated (Wotzlaw *et al*., 2007).

Table 3-17 CFP or YFP labeled vectors

N-terminal	Cards
pcDNA 6.2-N-CFP-DEST	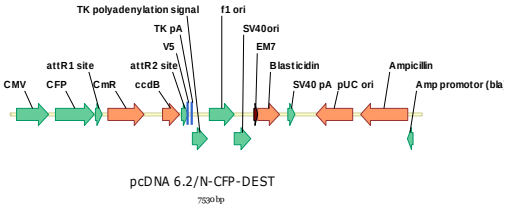
pcDNA 6.2-N-YFP-DEST	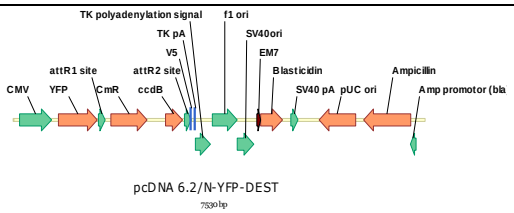
pExp-CFP-HIF-1α	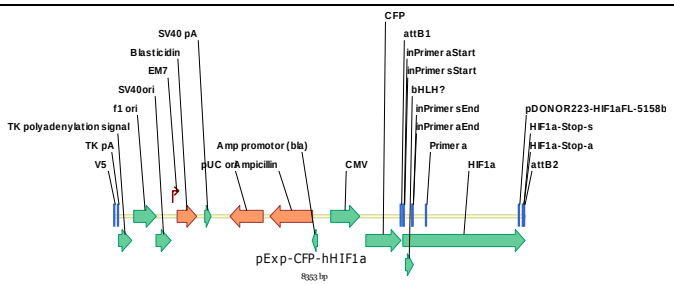
pExp-CFP-HIF-1αΔbHLH	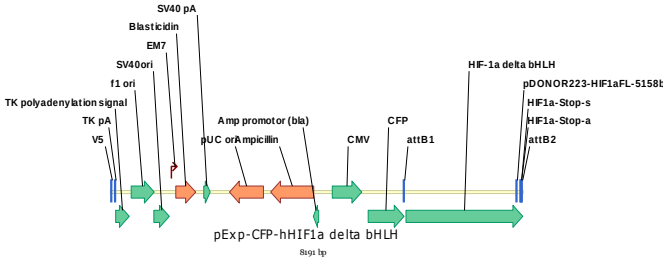
pExp-CFP-HIF-2α	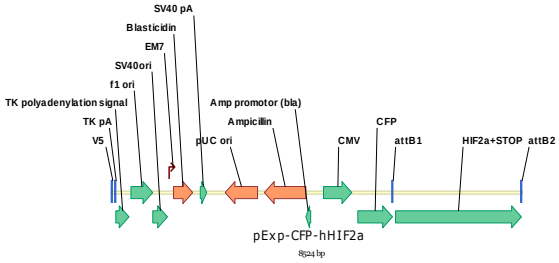

pExp-CFP-HIF-2αΔbHLH	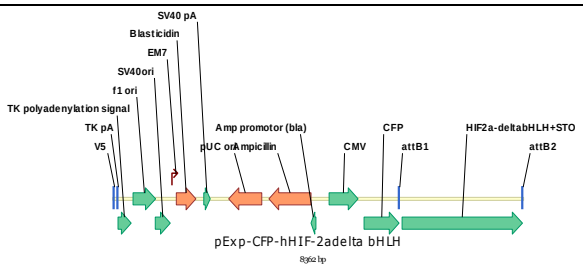
pExp-YFP-ARNT	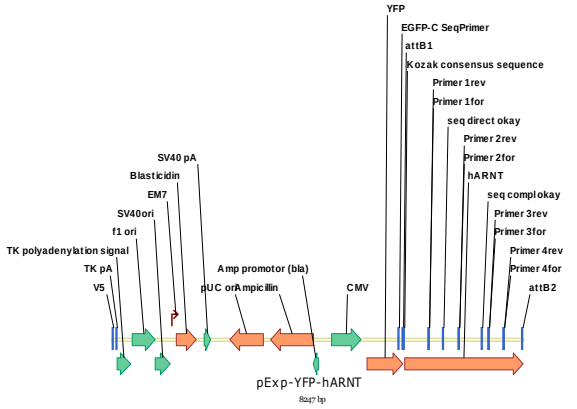
pExp-YFP-ARNTΔbHLH	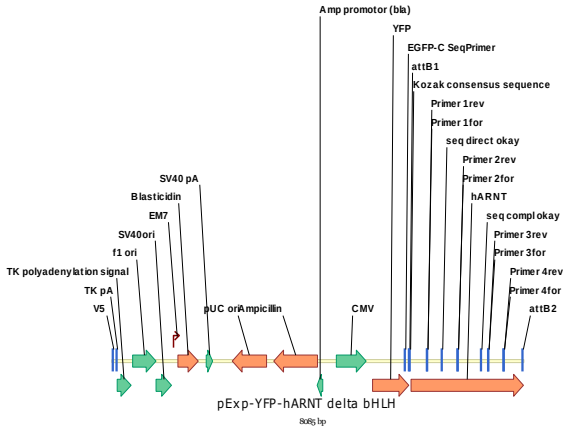
pExp-CFP-HIF-2αΔPASAB	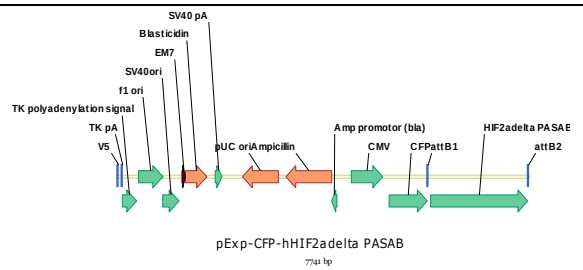
pExp-CFP-HIF-2αPASBm.	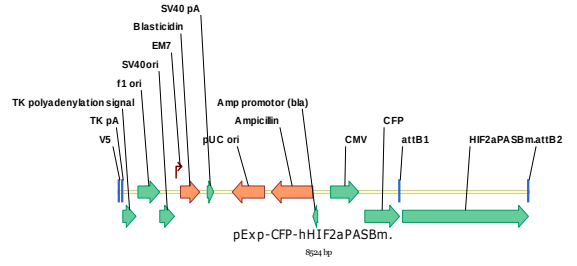

Equipment for FRET Study

For the FRET study, an inverted microscope (Axiovert 200M, Carl Zeiss MicroImaging GmbH, Germany) with a Nipkow Disc System (QLC100, Visitech International Ltd., USA) was applied. Two diode-pumped solid-state lasers (444 nm and 532 nm, Laser Crystal, USA) were used for specific excitation of fluorophores CFP and YFP. The laser light was coupled via an optical fiber cable into the system and focused on the sample chamber. Lasers came on the Nipkow Disc and a Multipec Microimager Dual View (Optical Insights, USA) to the CCD camera (Orca ERG, Hamamatsu, Japan). The Microimager Dual View served as a detection of two emission images (CFP and YFP channel) during the measurements. A special cell observation chamber (Luigs and Neumann GmbH, Germany) was used to keep the temperature constant. The gas concentrations were adjusted through gas mixer (MKS Instruments) to reach an expected gas concentration for normoxia or hypoxia.

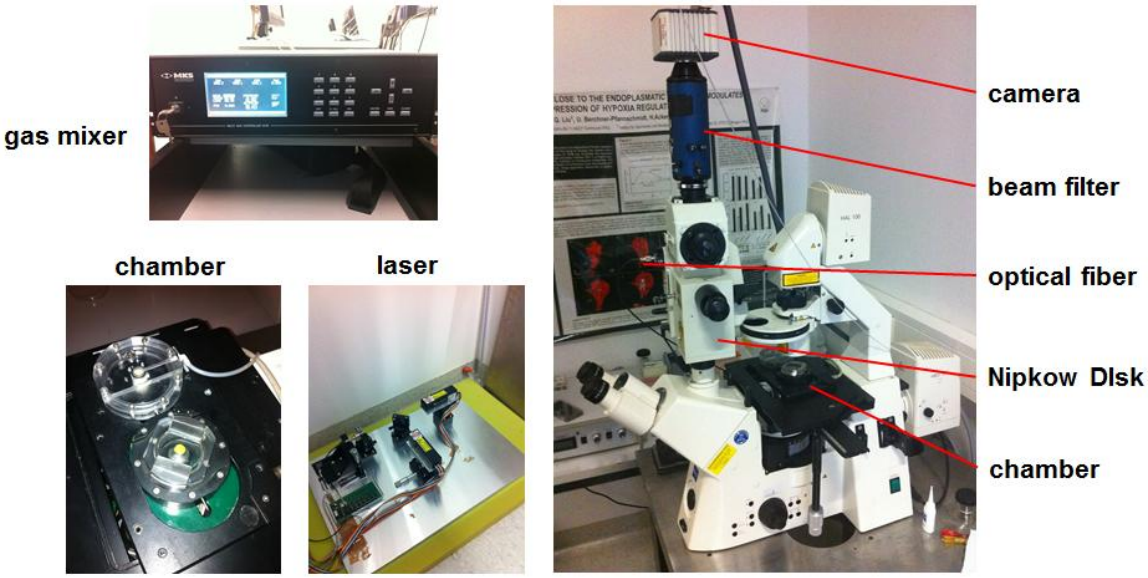

Fig. 3-12: Components of the microscopic system for FRET study

Two diode-pumped solid-state lasers with 444 nm and 532 nm lasers were produced in laser box, which was coupled with optical fiber cable into the microscope. Gas concentration was controlled by gas mixer and sent to the chamber, in which the FRET was studied in living cells.

Software for FRET Study

The software for FRET study called Anufis was programed by Dr. A. Bernadini and Dr. C. Wotzlaw (2009), updated by Dr. A. Bernadini using Javascript.

3.7 Laboratory Equipment

Table 3-18 Laboratory equipment and manufacturers

equipment	Manufacturers
autoclave	H+P Labortechnik GmbH
analytical balance, Pioneer	OHAUS
cool centrifuge, 5414R	Eppendorf
cool centrifuge, Biofuge fresco, Labofuge 400 R	Heraeus Instruments
electrophoresis system	BioRad
Fusion system	PEQLAB Biotechnologie
gel documentation for gel cutting	LTF Labortechnik
gel documentation for imaging	UVP
heat block: HLC TM 130-6, HLC HTM 130	Oehmen
hypoxia incubator, HERA cell 240	Heraeus Instruments
ice machine AF 10	Scotsman
incubator, Hera cell	Heraeus Instruments
Invivo$_2$ 400, Hypoxia Workstation	Russkin/Baker
light microscope, CK40	Olympus
luminometer, TD 20/20	Turner Instruments
PCR-machine: Tpersonal, Tprofessional	Biometra
PCR-machine: Mastercycler personal, Mastercycler	Eppendorf
pH-meter	Precisa
photometer, Epoch	BioTek
photo print for gel documentation	MITSUBISHI

pipetboy	Hirschmann Laborgeräte
shaker for 37 °C incubation	Edmund Bühler
shaker for Western blot	Oehmen
sterile bench, Hera safe	Heraeus Instruments
table centrifuge, 5415D	Eppendorf
vortexer, Vortex-Genie 2	Scientific Industries
water bath, GFL	Oehmen
Western blot, Mini Protean 3	Bio-Rad
water distillation system	Köttermann
Real-Time PCR detection system	Bio-Rad

3.8 Consumables and Chemicals

Table 3-19 Consumables and manufactures

Name	Manufacturers
culture flasks	Greiner
plastic consumables	Sarstedt, Eppendorf, Greiner
dishes for microscopy	Willcowells, Amsterdam
consumables for Western blot	Whatmann

The chemicals were purchased from Sigma-Aldrich, Merck, Fluka, Roth and Riedel-de Haën.

4. Results

4.1 FRET Study

FRET was applied for investigation of protein-protein interactions in U2OS cells. The FRET efficiency was recorded by Anufis version 1.20, 1.21 and 1.22. Data were analyzed in SigmaPlot 11.0 with nonlinear regression 'Exponential rise to Maximum'.

As a negative control, random FRET efficiency was measured after transfection of empty CFP and YFP (pcDNA 6.2-N-CFP-DEST and pcDNA 6.2-N-YFP-DEST) vectors. The low resulting 4.84 % plateau FRET efficiency indicated no significant FRET and distance > 10 nm between the fluophores was calculated according to the Förster formula (Fig. 3-10 A). Therefore, in case of in U2OS cells, positive FRET should be over 5 % FRET efficiency.

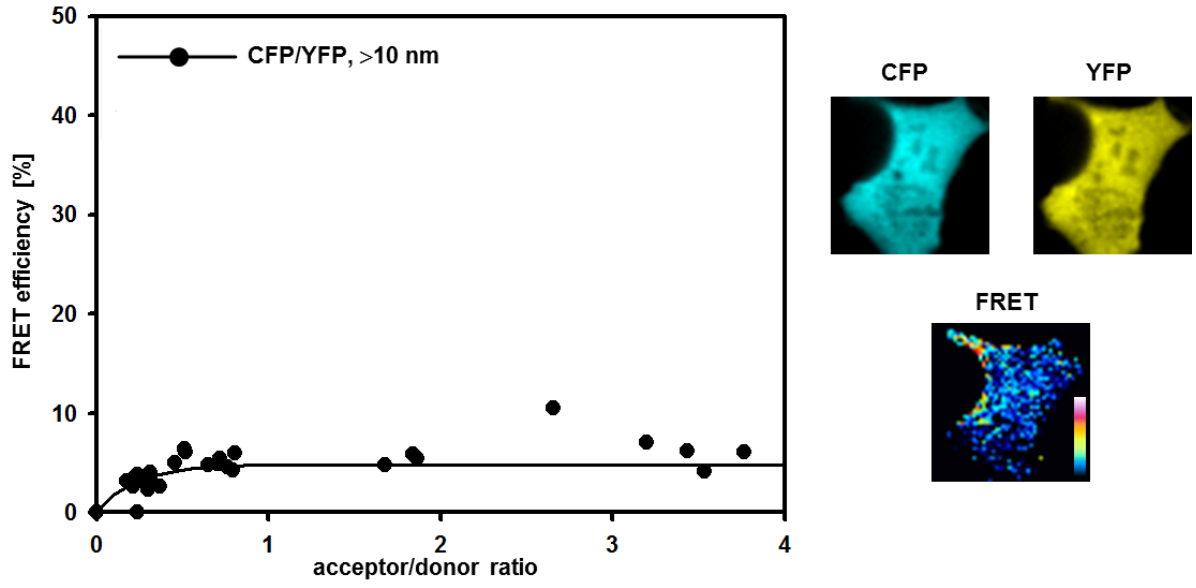

Fig. 4-1: Random FRET measured after CFP/YFP as negative control

Several cells had to be analyzed to get the plateau FRET efficiency, which is recorded against the acceptor/donor (YFP/CFP) ratio. After reaching the plateau FRET, the acceptor/donor

ratio does no longer influence FRET. In this case, 4.84 % FRET, representing a distance of more than 10 nm, was calculated.

The Role of the bHLH Domain in Heterodimerization

HIF-α/ARNT complexes have been described as the primary complexes in hypoxia which subsequent bind to DNA and regulate HIF-target genes (Wang *et al*., 1995). To detect potential differences between the assembly of the two heterocomplexes of HIF-1α or HIF-2α with ARNT, FRET was measured and distances of 6.0 nm between HIF-1α/ARNT (Fig. 4-2 A, solid curve) and 6.4 nm for HIF-2α/ARNT (Fig. 4-2 B, solid curve) were obtained indicating differences in the formation of these two highly similar complexes. To determine the contribution of the bHLH for heterodimerization, bHLH-deleted HIF fusion proteins (Fig. 2-4, middle section) were used. Interestingly, a distance of 6.4 nm was found for both HIF-1αΔbHLH/ARNTΔbHLH (Fig. 4-2 A, dashed curve) and HIF-2αΔbHLH/ARNTΔbHLH (Fig. 4-2 B, dashed curve) complexes. Compared with the wild type heterodimers, conclusion was made that bHLH domain is obviously not required for heterodimerization.

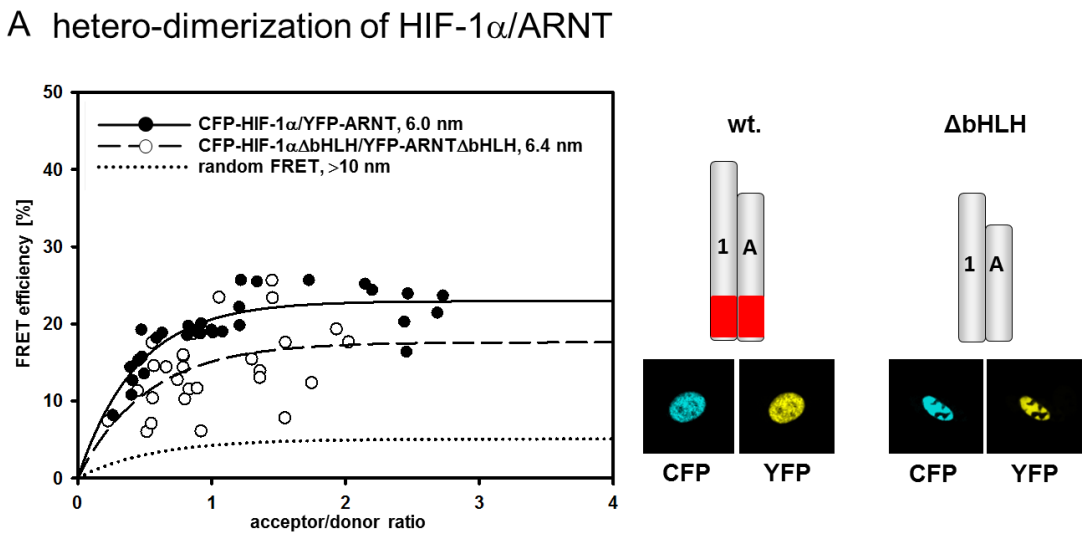

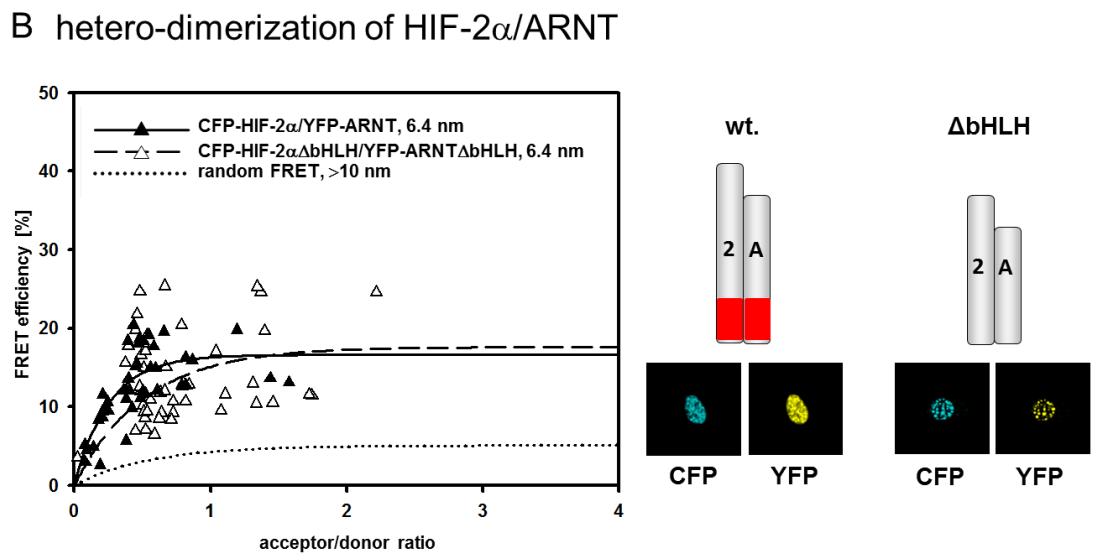

Fig. 4-2: bHLH study in heterodimerizatioin

All measurements were performed under normoxic condition. U2OS cells were transiently co-transfected with (A) HIF-1α/ARNT, HIF-1αΔbHLH/ARNTΔbHLH respectively and (B) HIF-2α/ARNT, HIF-2αΔbHLH/ARNTΔbHLH respectively. The dotted curves represent the random FRET measured after empty CFP and YFP.

Study of bHLH in Homodimerization

Among the bHLH-PAS proteins, homodimers have been recognized in several studies (Godlewski *et al*., 2006, Dioum *et al*., 2002 and Jones, 2004), and in the case of HIF proteins, homodimerization of ARNT was firstly described in 1995 (Sogawa *et al*., 1995). In this study, we observed the formation of homodimers of wildtype HIF-2α (Fig. 4-3 B, solid curve) with a distance of 6.1 nm between the subunits but also with HIF-2αΔbHLH (Fig. 4-3 B, dashed curve) with distance of 5.9 nm indicating that the bHLH domain is not required for HIF-2α homodimerization. Unexpectedly, neither the full-length nor the bHLH-deleted HIF-1α could form homodimers (Fig. 4-3 A, black and white dots under the random curve, distance > 10 nm), regardless of its high structural similarity compared with its isoform HIF-2α.

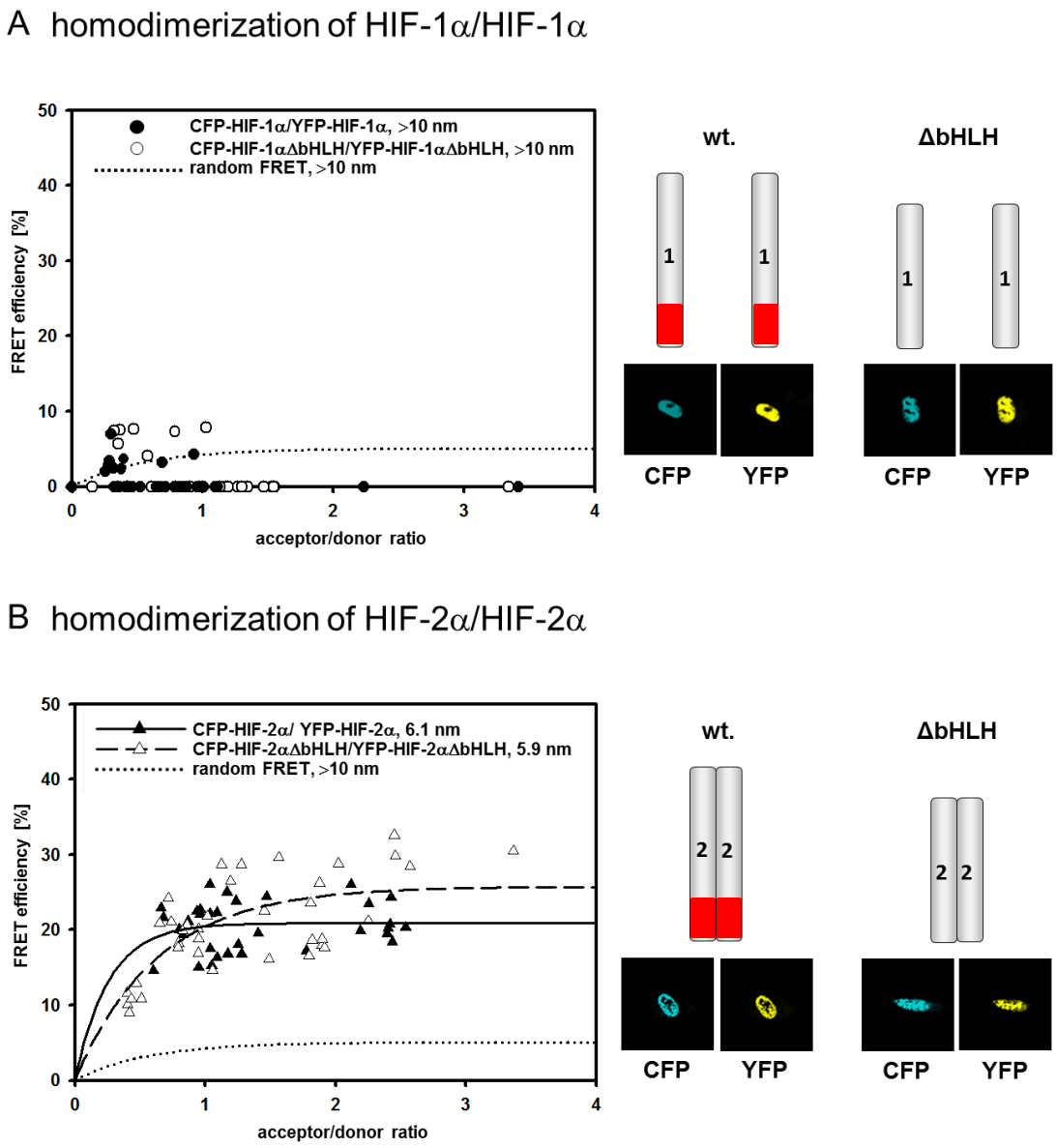

Fig. 4-3: Homodimerization of HIFα-units

All measurements were performed under normoxic condition. U2OS cells were transiently co-transfected with (A) HIF-1α/HIF-1α, HIF-1αΔbHLH/HIF-1αΔbHLH respectively and (B) HIF-2α/HIF-2α, HIF-2αΔbHLH/HIF-2αΔbHLH respectively. The dotted curves represented the random FRET measured after empty CFP and YFP.

Homodimerization of HIF-1α and HIF-2α

Interestingly, positive FRET with distances of 5.8 nm and 6.1 nm was observed on homodimer formation of the two isoforms HIF-1α/HIF-2α and HIF-1αΔbHLH/HIF-2αΔbHLH, respectively, which was not significantly influenced by the absence of bHLH (fig 4-4 B, solid and long dash curves).

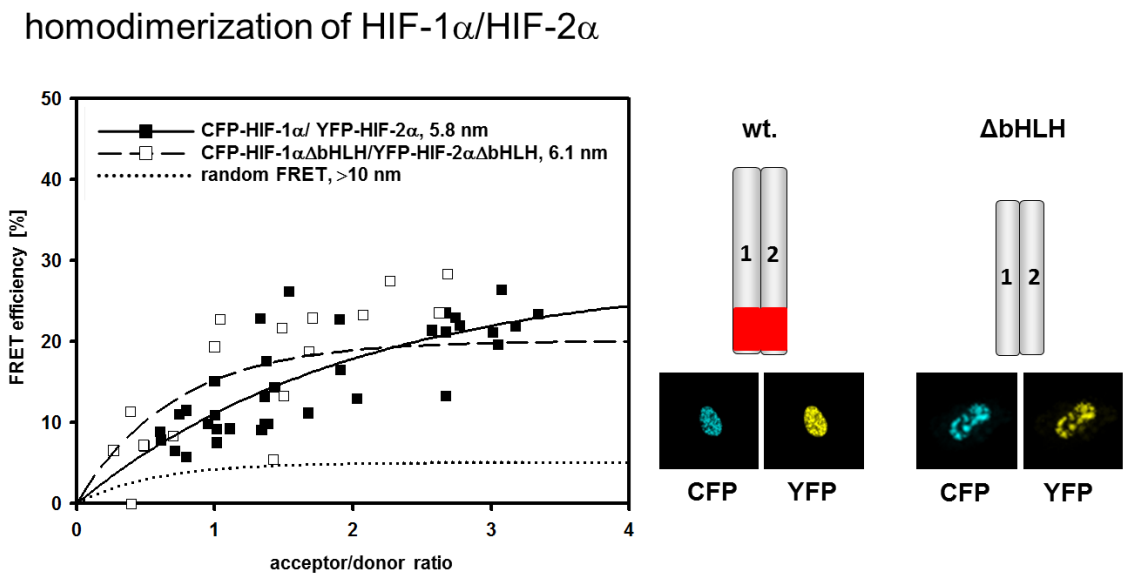

Fig. 4-4: Homodimer of HIF-1α/HIF-2α

Both measurements were performed under normoxic condition. U2OS cells were transiently co-transfected with HIF-1α/HIF-2α and HIF-1αΔbHLH/HIF-2αΔbHLH, respectively. The dotted curves represented the random FRET measured after empty CFP and YFP transfection.

The Role of the PAS Domain in Heterodimerization

To investigate the function of PAS during heterodimerization, a triple-point-mutation of PAS B-domain with minimal changes in the β-sheet backbone (Yang *et al.*, 2005) and a PAS AB-domain deletion of HIF-2α (Fig. 2-4, lower section) were generated. The PAS domain was proposed to be required for heterodimerization of HIF-2α/ARNT using its β-sheet interface (Card *et al.*, 2005). Herein the FRET analysis supported this hypothesis: neither the PAS B-triple-point-mutant, nor the PAS AB-deleted HIF-2α was able to heterodimerize with wildtype ARNT in normoxia (Fig. 4-5 A, black and white triangles were below random FRET). Furthermore, the PAS B-triple-point-mutant HIF-2α could not form a heterocomplex with wildtype ARNT even in hypoxia with 1 % O_2 (Fig. 4-5 B, black dots).

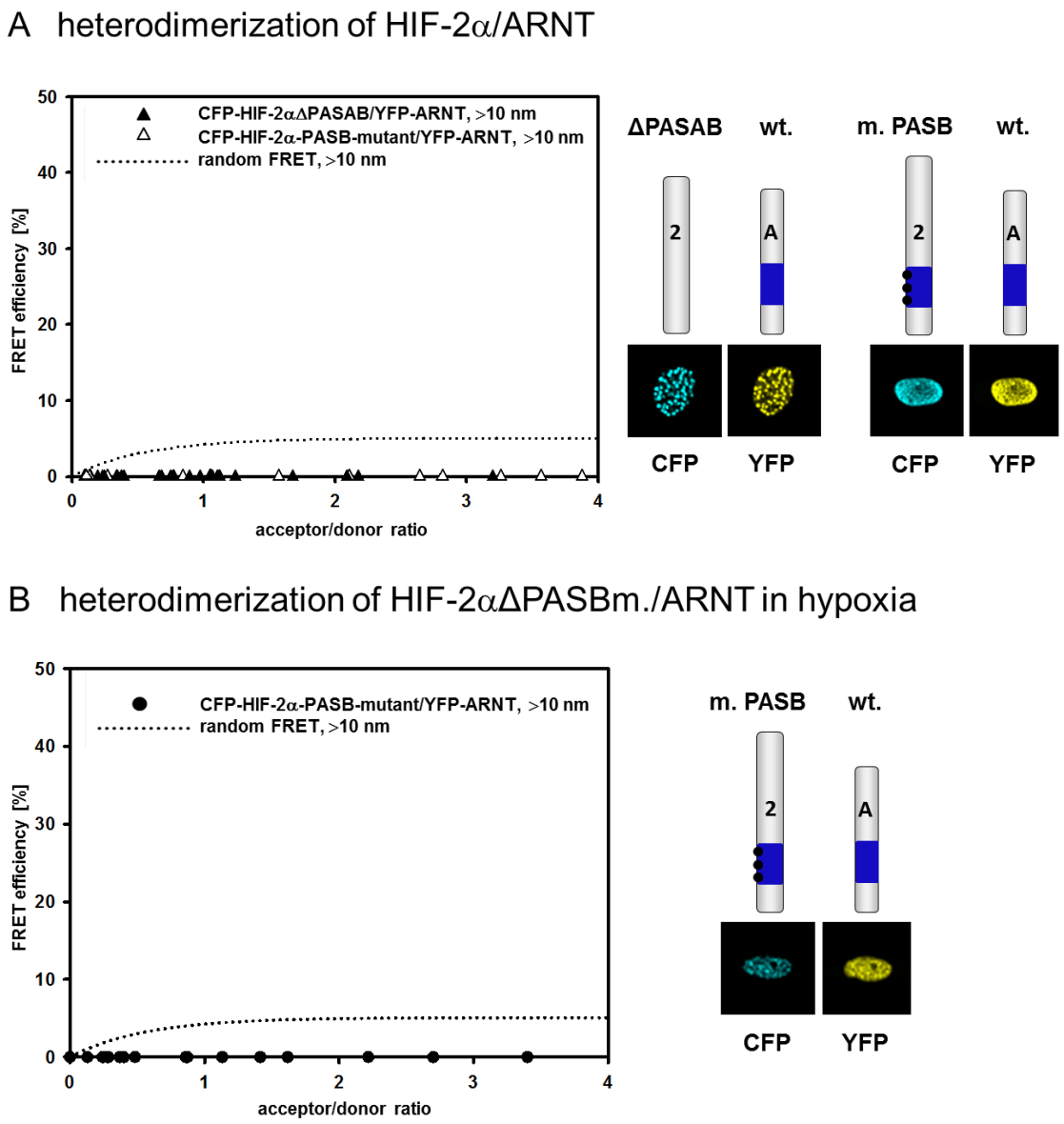

Fig. 4-5: PAS domain in heterodimerization

(A) Both measurements were performed under normoxic conditions. U2OS cells were transiently co-transfected with HIF-2αΔPASAB/ARNT and HIF-2αPASBm./ARNT, respectively. (B) After the co-transfection of HIF-2αΔPASAB/ARNT, FRET was determined under 1 % hypoxia. The dotted curves represented the random FRET measured after empty CFP and YFP.

The Role of PAS in Homodimerization

Moreover, no homodimerization was observed during the analysis of HIF-2αΔPASAB/HIF-2α and HIF-2αΔPASAB/HIF-1α (Fig. 4-6, black square and white triangle). These results support the notion that the B-domain of PAS is

essential for hetero- but also homodimerization via the exposed face of the β-sheet on the HIF-2α subunits.

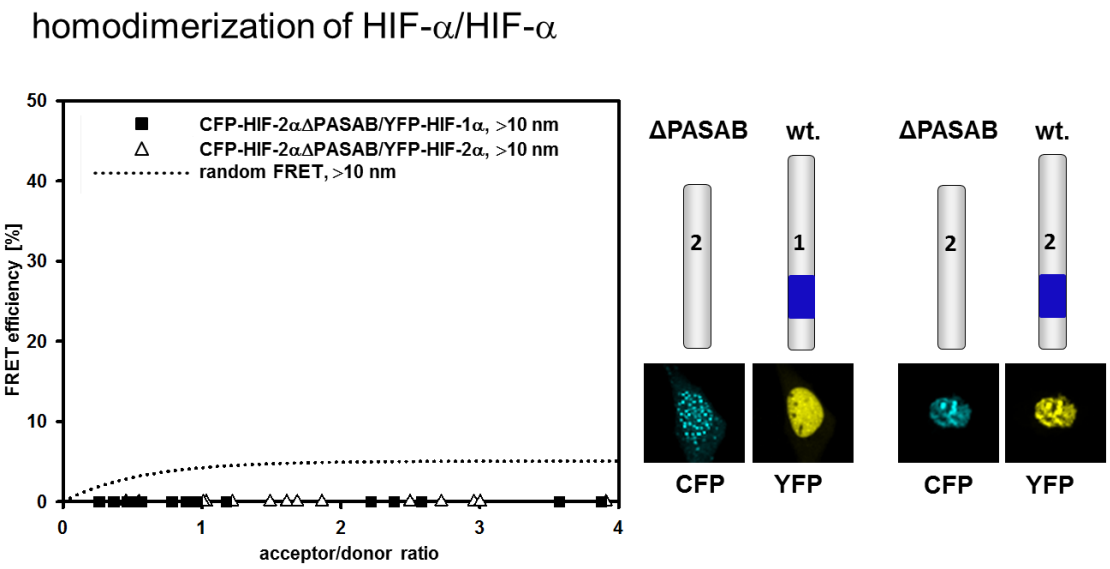

Fig. 4-6: The role of PAS in homodimerization

Both measurements were performed under normoxic condition. U2OS cells were transiently co-transfected with HIF-2αΔPASAB/HIF-2α and HIF-2αΔPASAB/HIF-1α, respectively. The dotted curves represented the random FRET measured after empty CFP and YFP.

4.2 Co-Immunoprecipitation

To confirm the assembly of homodimers of HIF-2α/HIF-2α (Fig. 4-3 B) and HIF-1α/HIF-2α (Fig. 4-4), co-immunoprecipitation was carried out. As the bait protein, HIF-2α was labeled with GAL4-tag for immunoprecipitation. As the prey proteins, HIF-2α and HIF-1α were tagged with HA for co-immunoprecipitation and further Western blot detection. As shown in Fig. 4-7, GAL4-HIF-2α was able to efficiently co-immunoprecipitate both HA-HIF-2α, and HA-HIF-1α, indicating the assembly of HIF homodimers, corresponding well with the FRET data.

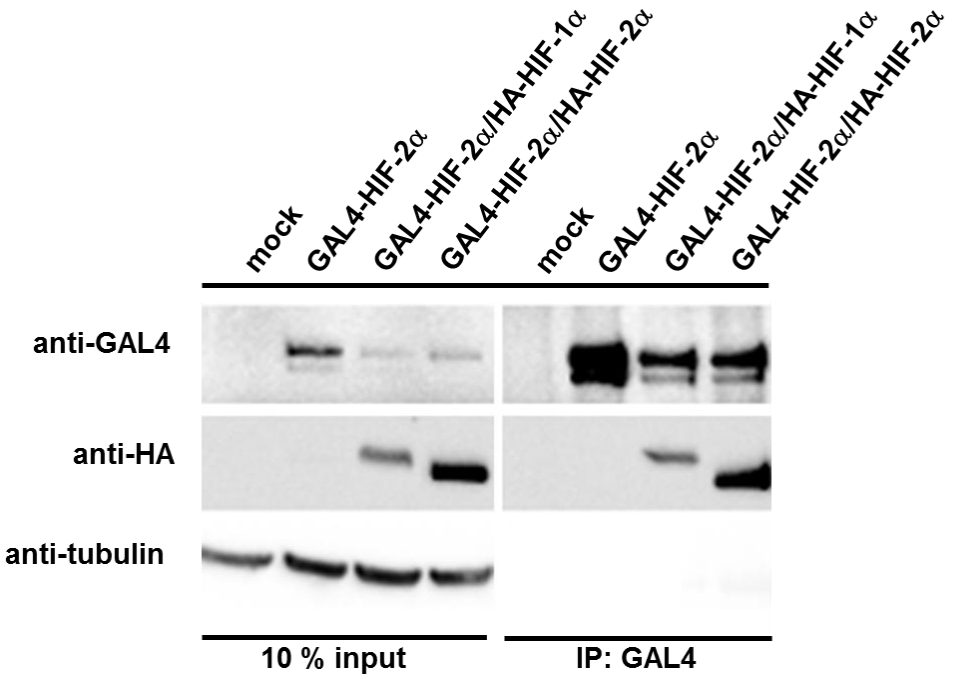

Fig. 4-7: Co-immunoprecipitation for HIF-2α/HIF-2α and HIF-2α/HIF-1α

For the co-immunoprecipitation, GAL4-HIF-2α was selected as precipitation protein, which efficiently coimmunoprecipitated the HA tagged HIF-2α and HIF-1α. Herein, 10 % input of the whole cell lysis protein. Single transfection of GAL4-HIF-2α served here as a negative control.

4.3 Electro-Mobility-Shift-Assay

To study potential DNA binding of HIF homo- or heterocomplexes, Electro-Mobility-Shift-Assays (EMSAs) were performed using the ^{32}P labeled W18 oligo (AGCTTGCCC**TACGTG**CTGTCTCAG) of the human erythropoietin gene enhancer containing the classical HIF binding site (HBS) TACGTG. As positive and negative controls, wild type and dKO U2OS (double knockdown of endogenous HIF-1α and ARNT, detail see results 4.4) were incubated both in normoxia and 1 % hypoxia for 6 h. As shown in Fig. 4-8, the typical hypoxia induced shifted complex was observed in hypoxia (lane 2) whereas dKO did not show the HIF-complex, neither in normoxia nor in hypoxia (lanes 3 vs 4).

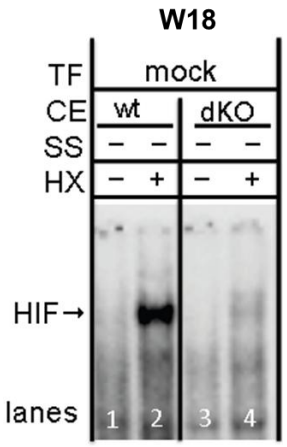

Fig. 4-8: Positive and negative controls for EMSA experiments

EMSA was carried out with oligo W18. TF, CE, SS and HX represent transfections (TF), cell extracts (CE), supershifts (SS) and hypoxia (HX) respectively. The mock was treated without any transfection.

Study of the bHLH Domain in DNA Binding

CFP or YFP labeled proteins were transfected in wt. U2OS for the following EMSA experiments, so that they could be distinguished from endogenous HIF complexes (without CFP and YFP) through their sizes. To identify the function of the bHLH during the DNA-binding, HIF-1α/ARNT and HIF-1αΔbHLH/ARNTΔbHLH were co-transfected into cells, respectively. As shown in Fig. 4-9, the overexpression of HIF-1α/ARNT allowed DNA bound complexes both in normoxia and hypoxia (lanes 5 and 6), which were supershifted with anti-HIF-1α (H^1, lane 7) and anti-ARNT (A, lane 8) antibodies, but not with a generic IgG (IgG, lane 9) antibody. On the contrary, no clear DNA-bound complex was observed after HIF-1αΔbHLH/ARNTΔbHLH co-transfection (lanes 10 and 11), due to the lack of the bHLH domain required for DNA binding. A slight trace in lane 11, which ran a little faster than complexes formed from exogenous overexpressed HIFs (lane 6 vs. lane 11), was the endogenous DNA-bound HIF-1α/ARNT heterocomplex.

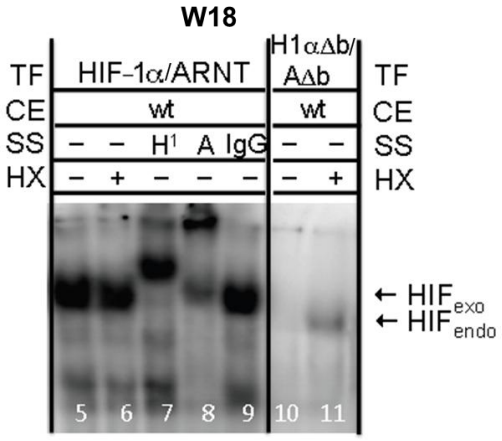

Fig. 4-9: The role of the bHLH domain for DNA binding

EMSA was carried out with oligo W18. TF, CE, SS and HX represented transfections (TF), cell extracts (CE), supershifts (SS) and hypoxia (HX) respectively. The supershifts were performed with anti-HIF-1α (H^1), anit-ARNT (A) and anti-IgG (IgG) antibodies.

DNA-Binding Study for Homodimer HIF-2α/HIF-2α

To study the DNA-binding of the homodimer HIF-2α/HIF-2α, both the asymmetric W18 oligo and the palindromic HBS within the Bnip3 promoter (ACGCGCCGC**ACGTG**CCACACGCAC) flanked by accessory E-box-like elements E1 and E2 (Hu *et al*., 2011) were used. As shown in Fig. 4-10, the exogenous overexpressed HIF-1α/ARNT was used as positive control complexes, which were shifted (lane 12) and supershifted with anti- HIF-1α (H^1, lane 13). The HIF-1αΔbHLH/ARNTΔbHLH co-transfection served here as negative control (lane 14, 15, 27 and 28). Although the HIF-2α formed homodimers (Fig. 4-3 and Fig. 4-7), this homodimer does not seem to bind to the asymmetric W18 HRE probe: Only endogenous HIF-1 complexes were observed under hypoxic conditions (lanes 17-21) which were supershifted with anti-HIF-1α (H^1, lane 18) and anti-ARNT (A, lane 19) antibodies but not anti-HIF-2α (H^2, lanes 20 and 21) antibodies.

Furthermore, no evidence of HIF-2α homodimer binding to DNA was found using the symmetric Bnip3 palindromic HBS probe: Only endogenous HIF-1

complexes were observed under hypoxic conditions (lanes 23-26) which were supershifted with anti-HIF-1α (H^1, lane 26) and anti-ARNT (A, lane 25) antibodies but not anti-HIF-2α (H^2, lane 24) antibodies. Herein, only faint DNA-bound complexes unrecognized by anti HIF-1α or anti ARNT antibodies were observed (lanes 21, 22, 28 and 29, red arrows), which might contain low affinity HIF-2α constituents. It is manifest that the HIF-1α heterodimer, but not the HIF-2α containing dimers, remain the predominant species bound to both asymmetric W18 and symmetric Bnip3 motif. In other words, HIF-2α preferably forms DNA-unbound homodimer, rather than to heterodimerize with endogenous ARNT.

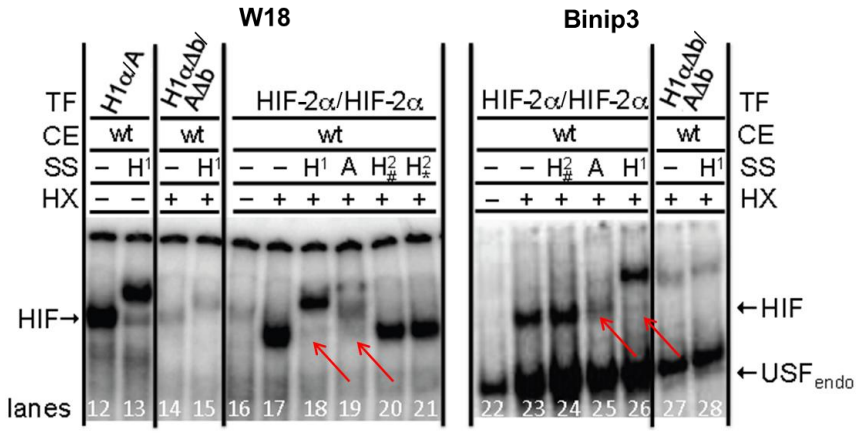

Fig. 4-10: DNA-binding study for homodimer of HIF-2α/HIF-2α

EMSA was carried out with oligo W18 and Bnip3. Transfections (TF), cell extracts (CE), supershifts (SS) and hypoxia (HX) respectively. The supershifts were performed with anti-HIF-1α (H^1), anti-HIF-2α (H^2) and anit-ARNT (A) antibodies.

DNA-Binding Study for Homodimer HIF-1α/HIF-2α

As shown in Fig. 4-11, only very weak complexes, supershifted with anti-HIF-1α (H^1, lane 31) and anti-ARNT (A, lane 32) antibodies but not anti-HIF-2α (H^2, lane 33) antibodies, were observed in the HIF-1α/HIF-2α homodimer test, indicating the endogenous HIF-1α/ARNT heterocomplex. However, compared e.g. Fig. 4-10 (lanes 17-21), these HIF-1α/ARNT complexes were apparently

weaker, indicating that HIF-2α overexpression inhibited HIF-1α to heterodimerize with ARNT by forming a DNA unbound complex HIF-1α/HIF-2α.

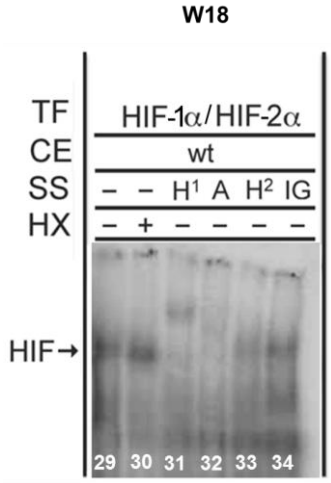

Fig. 4-11: DNA-binding study for homodimer HIF-1α/HIF-2α

EMSA was carried out with oligo W18 and Bnip3. Transfections (TF), cell extracts (CE), supershifts (SS) and hypoxia (HX) respectively. The supershifts were performed with anti-HIF-1α (H^1), anti-HIF-2α (H^2), anit-ARNT (A) and anti-IgG (IgG).

The Role of the PAS Domain for DNA Binding

To study the role of the PAS domain the HIF-2α-PAS B-triple-point-mutant (HIF-2αPASBm.) was used. Neither under normoxia (Fig. 4-12, lanes 35 to 37) nor under hypoxia (Fig. 4-12, lanes 38 to 40), exogenous cotransfection of HIF-2αPASBm./ARNT led to the formation of exogenous DNA bound complexes, whereas only endogenous HIF-1 complexes (endogenous HIF-1α with endogenous/exogenous ARNT) were observed in hypoxic conditions (Fig. 4-12, lanes 38-40).

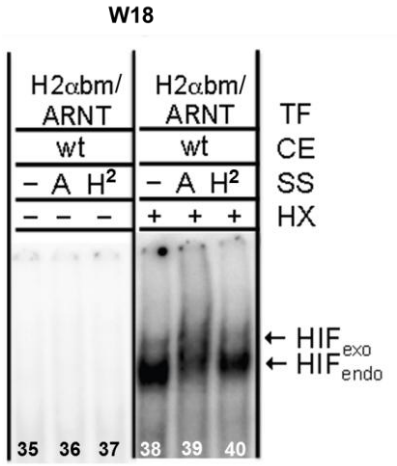

Fig. 4-12: PAS study in DNA binding

EMSA was carried out with oligo W18 and Bnip3. TF, CE, SS and HX represented transfections, cell extracts, supershifts and hypoxia respectively. The supershifts were performed with anti-HIF-2α (H^2) and anit-ARNT (A).

4.4 Luciferase Reporter Gene Assay and Western Blot

Using the pH3SVL plasmid in which 3 HRE elements control luciferase reporter gene expression, the transcriptional activity of HIF assemblies which included the classic heterocomplexes of HIF-α/ARNT and newly identified homocomlexes of HIF-α/HIF-α was studied. The U2OS cells belong to the common somatic cells, indicating the absence of endogenous HIF-2α (Wiesener *et al*., 2003), however they contain endogenous HIF-1α and ARNT. To avoid interference by endogenous HIF complexes, endogenous HIF-1α and ARNT were knocked down with sh-HIF-1α and sh-ARNT in U2OS (dKO U2OS were generated from Dr. U Brockmeier, Essen, Germany). The knockdown efficiency (over 80 %) was confirmed and assessed by Western blot analysis (Fig. 4-13 B): Little HIF-2α and only residual HIF-1α and ARNT were observed both in normoxia and in hypoxia compared with wild type U2OS. Reasonably, the transcriptional activity of the dKO U2OS ceased substantially compared with the wild type U2OS both in normoxia and in hypoxia, with the ‘clean

background' (Fig 4-13 A). These dKO U2OS cells were applied for the reporter gene assay.

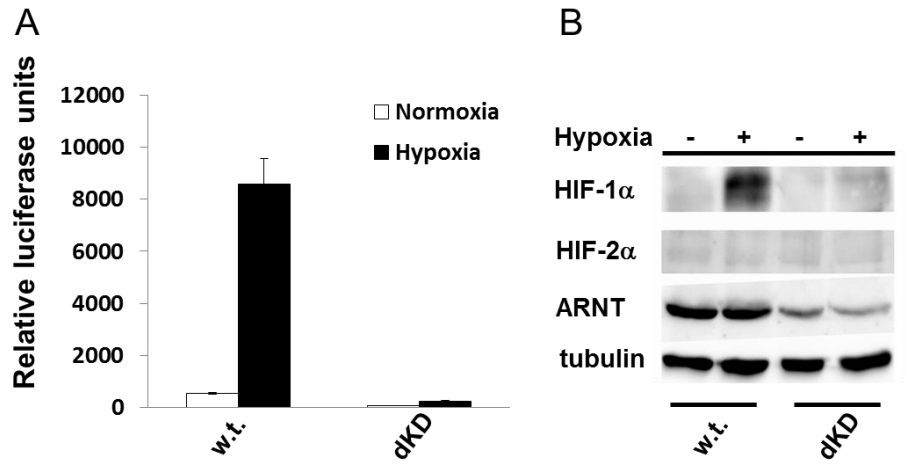

Fig. 4-13: Double knockdown of endogenous HIF-1α and ARNT in U2OS

(A) To investigate the transcriptional activity, a luciferase reporter gene assay was carried out in dKO U2OS cells, which were transiently transfected with pH3SVL plasmid reporter gene and incubated under normoxic or hypoxic (1 % O_2) conditions for 6 h. The values represent the average luciferase activity of three replicates with the bars indicating standard error. (B) The Western blot provided rough expression levels.

Reporter Gene Assay after Single Transfection

For single transfection, empty CFP and YFP served as negative controls. HIF-1α, HIF-1αΔbHLH, HIF-2α, HIF-2α and HIF-2αΔbHLH were single-transfected in dKO U2OS cells. With the absence of endogenous ARNT, all of the single transfections apparently resulted in low activity of the reporter gene (values under 1000 units) both in normoxia and in hypoxia (Fig. 4-14 A). According to the FRET study (Fig. 4-3 B) and co-immunoprecipitation (Fig. 4-7), homodimer of HIF-2α was confirmed. However, no increase in transcription of the reporter gene was observed (Fig. 4-14 lanes 5 and 6), corresponding well the EMSA data (Fig. 4-10). Western blots of extracts from the cells confirmed efficient transfection of the respective single transfected HIF-subunits and the absence of endogenous HIF proteins (Fig. 4-14 B).

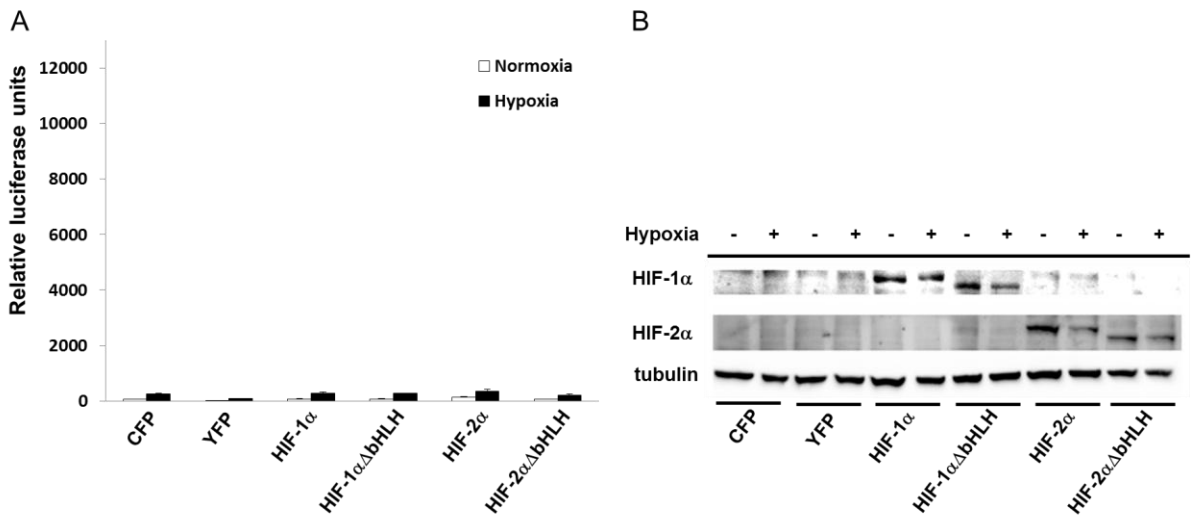

Fig. 4-14: Reporter gene assay after single transfection

(A) HIF-1α, HIF-1αΔbHLH, HIF-2α, HIF-2α and HIF-2αΔbHLH were single-transfected in dKO U2OS cells and incubated under normoxic or hypoxic (1 % O_2) conditions for 6 h. The values represent the average luciferase activity of three replicates with the bars indicating standard error. (B) The Western blot provided rough expression levels.

Reporter Gene Assay after Co-Transfection

Co-transfections were performed with HIF-1α/ARNT, HIF-1αΔbHLH/ARNTΔbHLH, HIF-2α/ARNT, HIF-2αΔbHLH/ARNTΔbHLH, HIF-1α/HIF-2α and HIF-1αΔbHLH/HIF-2αΔbHLH, respectively. It is obvious that significant transcriptional activity was observed only for two wild type heterocomplexes of HIF-1α/ARNT and HIF-2α/ANRT (Fig. 4-15 A, lanes 1 and 3). Compared with the wild type complex, the bHLH-deleted complexes provided little activity (Fig. 4-15 A, lanes 2 and 4 compared with lanes 1 and 3), indicating that the DNA-binding required the bHLH domain. Additionally, the heterocomplexes of HIF-2α generally provided higher values than HIF-1α heterocomplexes in the case of U2OS cells (Fig. 4-15 A, lane 2 compared with lanes 1). Although the homodimers of HIF-1α/HIF-2α were observed by FRET and co-immunoprecipitation (Fig. 4-4 and Fig. 4-7), no considerable activity was observed for complexes of HIF-1α/HIF-2α or HIF-1αΔbHLH and HIF-2αΔbHLH (Fig. 4-15 A, lanes 5 and 6), corresponding well the EMSA data of

Fig. 4-15. Appropriate expression levels were confirmed by Western blot (4-15 B).

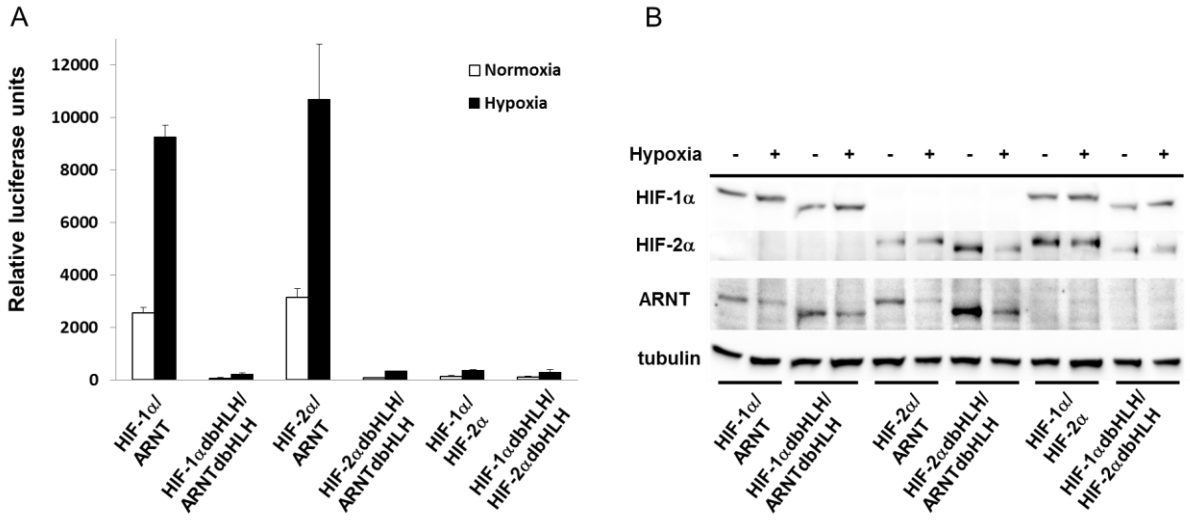

Fig. 4-15: Reporter gene assay after co-transfection

(A) HIF-1αΔbHLH/ARNTΔbHLH, HIF-2α/ARNT, HIF-2αΔbHLH/ARNTΔbHLH, HIF-1α/HIF-2α and HIF-1αΔbHLH/HIF-2αΔbHLH were co-transfected in dKO U2OS cells and incubated under normoxic or hypoxic (1 % O_2) conditions for 6 h. The values represent the average luciferase activity of three replicates with the bars indicating standard error. (B) The Western blot provided rough expression levels.

PAS Study Using Reporter Gene Assay

For PAS study, assemblies of HIF-2αPASBm./ARNT, HIF-2αΔPASAB/ARNT, HIF-2αΔPASAB/HIF-1α and HIF-2αΔPASAB/HIF-2α were co-transfected in dKO U2OS cells. Interestingly, transcriptional activity was observed for the HIF-2αPASBm. complex (Fig. 4-16 A), albeit on a substantially lower level when compared with wild type complex HIF-2α/ARNT (Fig. 4-15 A, lane 3). According to the FRET data of Fig. 4-5 and 4-6, no dimerization was observed for HIF-2α homo- or heteroassemblies in case of the absence of whole PAS domain. Evidently, no activity above background of HIF-2αΔPASAB/ARNT, HIF-2αΔPASAB/HIF-1α or HIF-2αΔPASAB/HIF-2α was detected (Fig. 4-16 A, lanes 2 ,3 and 4), indicating the requirement of the whole PAS domain for hetero- and homodimerization, specially the requirement of the wild type PAS B-domain for the full transcriptional activity.(Yang *et al*., 2005). Again, the

expression levels of the respective HIF-subunits were confirmed by Western blot (Fig. 4-16 B).

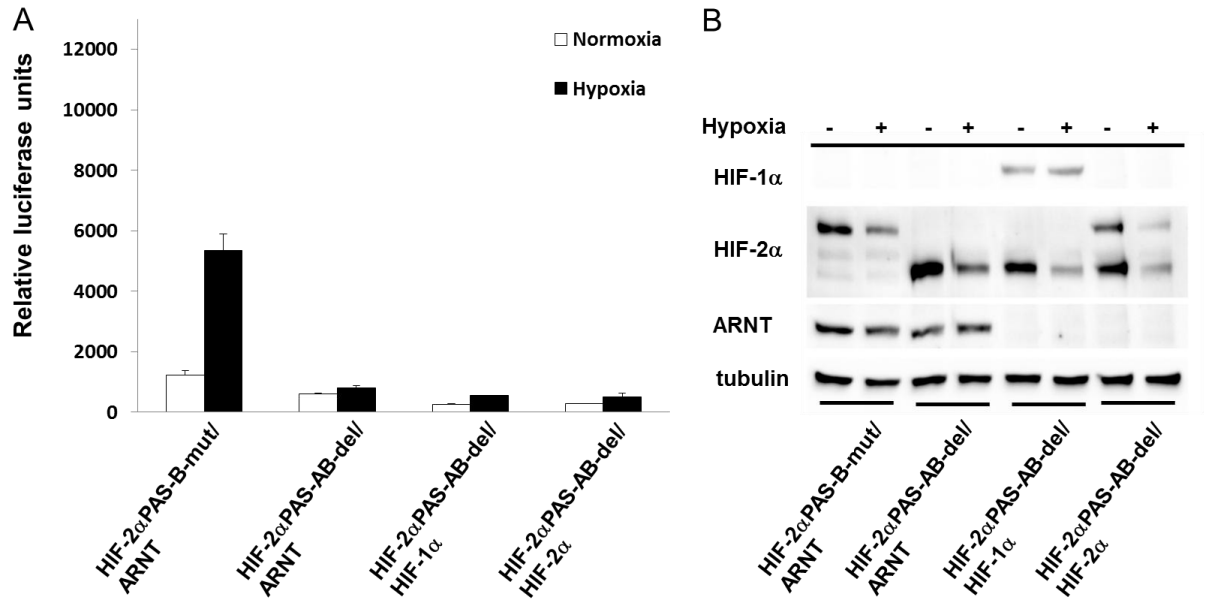

Fig. 4-16: PAS study using reporter gene assay

(A) HIF-2αPASBm./ARNT, HIF-2αΔPASAB/ARNT, HIF-2αΔPASAB/HIF-1α and HIF-2αΔPASAB/HIF-2α were co-transfected in dKO U2OS cells and incubated under normoxic or hypoxic (1 % O_2) conditions for 6 h. The values represent the average luciferase activity of three replicates with the bars indicating standard error. (B) The Western blot provided rough expression levels.

4.5 CA9-Quantification Using Real Time PCR

The homodimer of HIF-1α/HIF-2α was confirmed by FRET data (Fig. 4-3 B) and co-immunoprecipitation (Fig. 4-7), however provided no DNA-binding (Fig. 4-10) and subsequent transcription activity (Fig. 4-14 A). This allowed us to considerate the physiological meaning of the homodimer complexes. To address this question, a HIF-1α specific target gene carbonic anhydrase 9 was used to identify the meaning of HIF-1α/HIF-2α using real time PCR experiment. 2 µg ANRT was first transfected into wild type U2OS cells to ensure sufficient dimerization partner for both HIF-1α and HIF-2α to form heterocomplexes. After 6 h incubation in 1 % hypoxia, accumulated endogenous HIF-1α formed

heterocomplex of with ARNT. A titration of HIF-2α against HIF-1α/ARNT complex was carried out by starting from 0 to 1.4 µg in steps of 0.2 µg plasmid amounts. Surprisingly, the CA9 mRNA expression level decreased almost 50 % already in the early stage of the 0.2 µg HIF-2α transfection, which continued until CA9 expression level reduced to about 20 %. With respect to the EMSA results in Fig. 4-11, HIF-2α was proved to inhibit the heterodimerization of HIF-1α/ARNT by forming a DNA unbound complex HIF-1α/HIF-2α. Combining these results, further conclusion was made that HIF-2α in non-DNA binding HIF-1α/HIF-2α complexes might compete with ARNT for HIF-1α, which caused the reduction of HIF-1α/ARNT dependent gene expression like CA9.

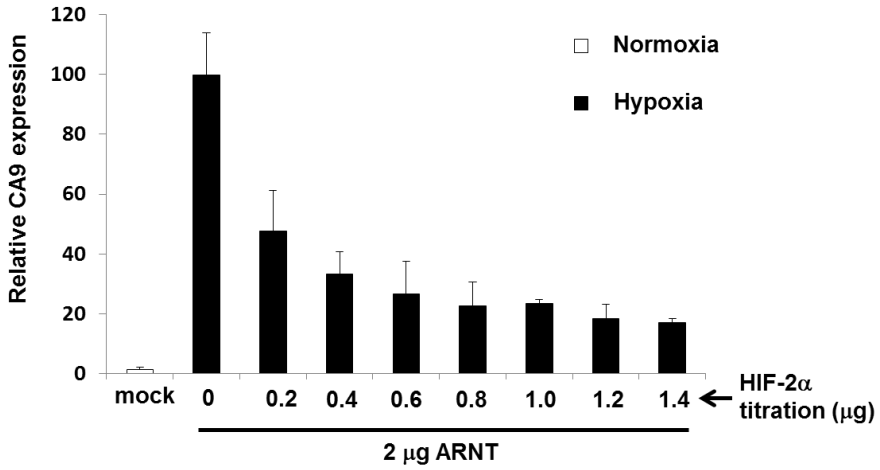

Fig. 4-17: CA9-quantification using real time PCR

Figure provided the mRNA level of carbonic anhydrase 9 using real time PCR. After transfection of ARNT, titration of HIF-2α was performed against endogenous HIF-1α induced in 1 % hypoxia. The values represent the average units of three replicates with the bars indicating standard error.

5. Discussion

Hypoxia-inducible factors are today well known bHLH-PAS transcription factors, which provide a signaling pathway to sense hypoxia and respond to balance the O_2 availability in all mammalian cells (Semenza, 2001). As a potential target for therapeutic approach to hypoxic tissue disease, the transcriptional pathway of HIF is meticulously investigated. As a result, some small molecules interfering either with HIF-subunit dimerization or HIF-DNA binding have identified and are currently tested for applicability (Key *et al*., 2009, Choi *et al*., 2009, Lee *et al*., 2009, van de Sluis *et al*., 2010, Vinson, 2005 and Scheuermann *et al*., 2009). To provide some basic insight into HIF complex assembly, this study aimed at examining the different contributions of bHLH and PAS domains to both dimerization and DNA-binding. Furthermore, we also examined complex formation by the highly similar isoforms HIF-1α and HIF-2α with ARNT. By applying modern confocal microscopic FRET, I was able to elucidate protein-protein interaction of HIF subunits directly in living cells, to a great extend mimicking physiological conditions. Our data may provide a new view in the study of HIF activation.

5.1 The Role of the bHLH Domains

bHLH proteins are well conserved and widespread in mammalian cells (Murre *et al*., 1994). As a member of this protein family, hypoxia inducible factor belongs to the class of bHLH proteins which are ubiquitously expressed and can form either homo- and/or heterodimers (Murre *et al*., 1989). The N-terminal region, which consists of basic residues, was identified to allow the protein to bind to DNA: Deletion of the conserved basic residues abrogates DNA binding (Davis *et al*., 1990). This finding was fully supported by the present study: In the Electro-Mobility-Shift-Assay, no clear DNA-bound complex was observed

after HIF-1αΔbHLH/ARNTΔbHLH co-transfection (Fig. 4-9, lanes 10 and 11), due to the lack of the basic region of the bHLH domain. Due to the failure to bind to DNA, the determination of transcriptional activity using the luciferase reporter gene assay revealed loss of this function (Fig. 4-15 A, lanes 2 and 4). The second HLH region characterized by hydrophobic residues is described to be involved in homo- and/or heterodimerization. Insertion of proline residues or mutation of the conserved hydrophobic residues obliterated the ability to form dimers (Davis *et al*., 1990). However, in the case of HIF proteins (both HIF-1 and HIF-2), no substantial difference was observed by comparing the wildtype and bHLH-deleted complexes in the heterodimerization study using FRET (Fig. 4-2 A and B). It should be noted that the bHLH domain was neither required for homodimerization (Fig. 4-3 B or Fig. 4-4). As potential explanation it is possible that in the case of bHLH and PAS domain combining proteins like HIF, the PAS might be more dominant both for homo- and heterodimerization.

5.2 Functions of the PAS Domains

Hypoxia inducible factors belong to the largest class of PAS proteins, which is known as the bHLH-PAS family consisting of bHLH, PAS-A, PAS-B and and C-terminal transactivation domain (Letunic *et al*., 2006). In the previous discussion of bHLH, my results emphasize that the bHLH domain contributes to the DNA-binding with its basic region, however, it does not substantially confer dimerization with its helix-loop-helix domain, implying that HIF dimerization might require the PAS domain with its β-sheet interfaces defining the formation of specific heterodimerization (Erbel *et al*., 2003, Card *et al*., 2005, Yang *et al*., 2005, Scheuermann *et al*., 2009 and Zhu *et al*., 2012). To investigate the function of the PAS domain during dimerization, a triple-point-mutation of the PAS B-domain with minimal changes in the β-sheet backbone (Yang *et al*., 2005) and a PAS AB-domain deletion of HIF-2α (Fig. 2-4, lower section) were used for FRET. Neither homo- nor heterodimerization was found using the

protein with mutational changes in the PAS domain (Fig. 4-5 A, B and Fig. 4-6), indicating that the β-sheet interfaces were indeed required both for homo- and heterodimerization. No further DNA bound heterocomplexes were observed in HIF-2αPASBm./ARNT (Fig. 4-12). Interestingly, some transcriptional activity was observed for the HIF-2αPASBm. complex (Fig. 4-16 A, lane 1), albeit on a substantially lower level when compared with wild type complex HIF-2α/ARNT (Fig. 4-15 A, lane 3), while no activity above background of HIF-2αΔPASAB/ARNT was detected (Fig. 4-16 A, lane 2). This might indicate the requirement of the whole PAS domain for heterodimerization, specially the requirement of the wild type PAS B-domain for the full transcriptional activity (Yang *et al*., 2005). In addition, unlike the HIF-2α (Fig. 4-3 A), HIF-1α could not form homodimers (Fig. 4-3 B). Thus, it is tempting to speculate that the characteristics of β-sheet interfaces involving homo- and heterodimerization are very important and that the β-sheet in HIF-1α might be too short to form homodimers.

5.3 The HIF-2α Homodimer

Heterodimerization of HIF-1α and its isoform HIF-2α with the constitutive ARNT is required for HIF transcriptional activity. Using the common β-sheet interfaces, PAS domains lead to the heterodimer formation (Card *et al*., 2005). As discussed in discussion 5.2, the β-sheet interfaces might however contribute differently to the homodimer formation between HIF-1α and HIF-2α: only HIF-2α homodimers were observed in FRET (Fig. 4-3 B) and confirmed by co-immunoprecipitation (Fig. 4-7). Interestingly, however, they shared no DNA-binding with heterodimers regardless whether the asymmetric W18 HIF binding site (HBS) as part of the erythropoietin enhancer or the palindromic HBS from Bnip3 (Fig. 4-10) were used, and apparently showed very low transcriptional activity (Fig. 4-14, lane 5).

It is widely recognized that HIF-1 and HIF-2 colocalize in tissues like the kidney where the typical heterodimerization pathway with ARNT is shared both for HIF-1α and HIF-2α to induce their specific or common target genes (Fig. 5-1). Simultaneously, however, one may speculate about a competitive behavior: HIF-2α transcriptional activity might be suppressed by forming nonfunctional HIF-2α homodimers (Fig. 5-2). This notion might be the cause for the primary activation during the acute phase of hypoxic adaptation of HIF-1α and the secondary dominant activation during the chronic phases of HIF-2α (Holmquist-Mengelbier *et al*., 2006). Furthermore, the homodimer might prevent the HIF-2α from translocation, hydroxylation and subsequent degradation, although the underlying details require additional study and proof.

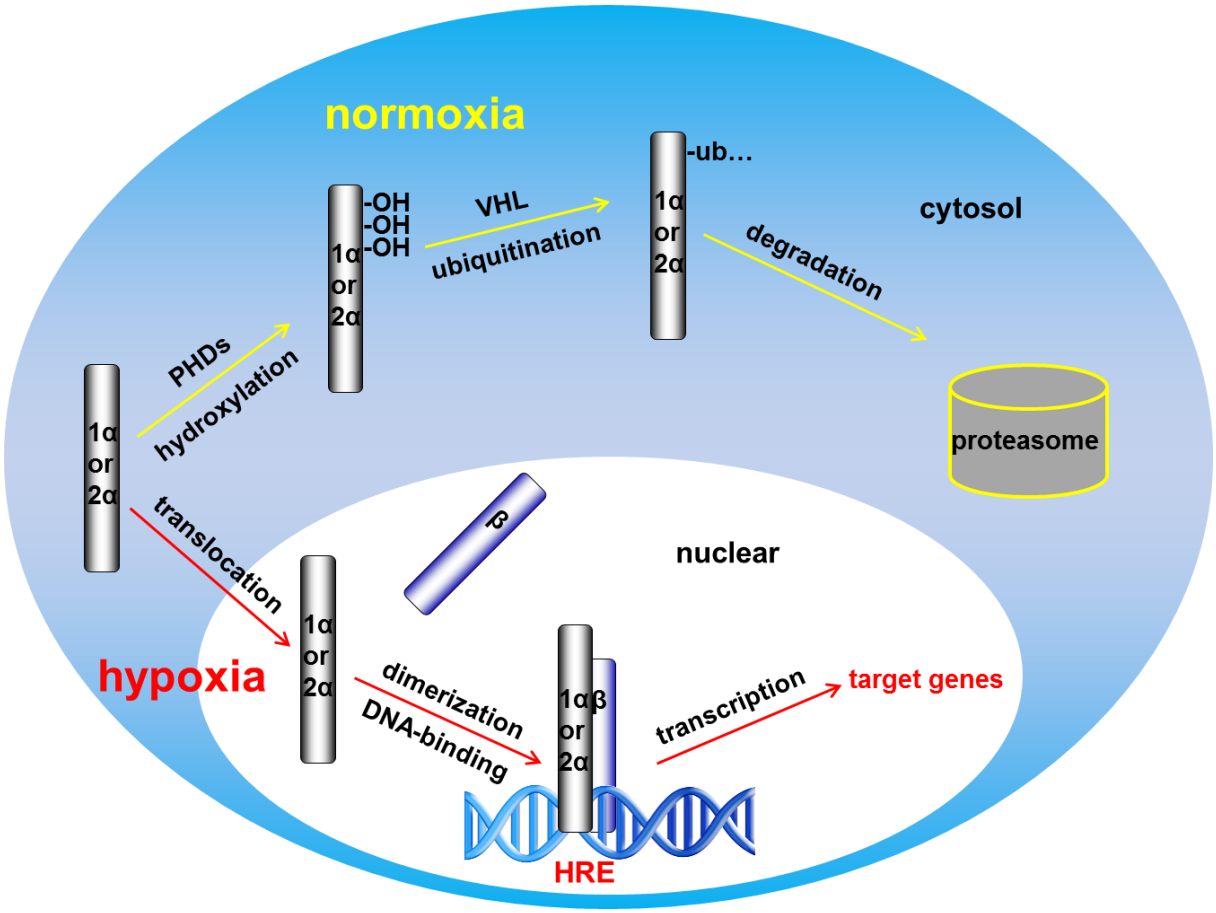

Fig. 5-1: "Classic" heterodimeric HIF-1α and HIF-2α mediated pathway in cells

HIF-αs accumulate in hypoxia and translocate into nuclear to dimerize with ARNT. Heterocomplex bind to HRE of DNA to induce HIF target genes. In normoxia, α-subunits can be rapidly hydroxylated, unbiquitinylated and proteasomal degraded.

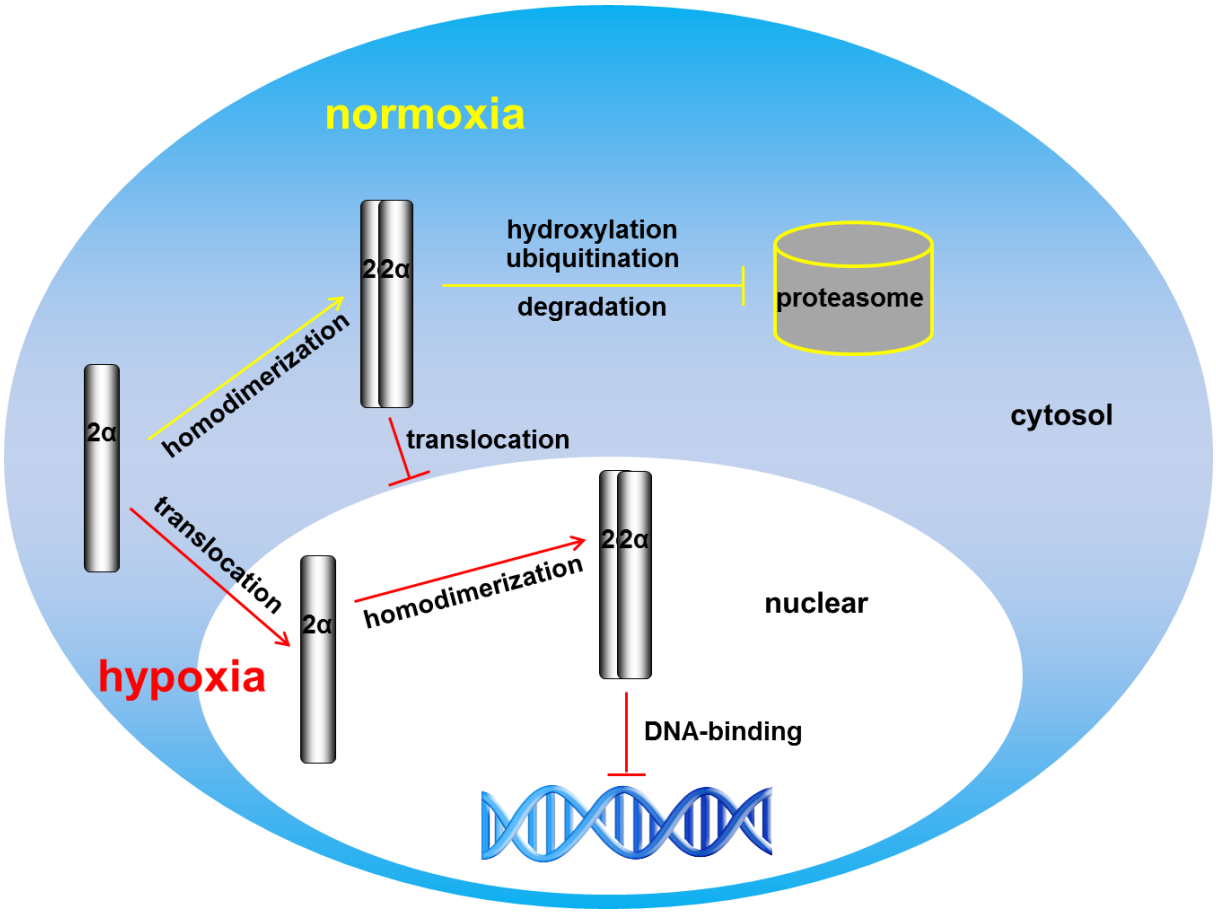

Fig. 5-2: HIF-2α suppressed its activity by forming homodimer

Within the nucleus, the HIF-2α transcriptional activity was suppressed by forming HIF-2α homodimers. The homodimer might also prevent the translocation and proteasomal degradation of HIF-2α.

5.4 The Role HIF-1α/HIF-2α Homodimers

Since the identification of the two isoforms HIF-1α and HIF-2α a number of studies about their similarity have been performed, also aimed at defining specific roles. Both of them are highly conserved at the protein level, sharing a similar protein structure and several common target genes like VEGF (Loboda *et al.*, 2010). However, clear cell renal carcinoma proliferation is retarded by HIF-1α, but induced by HIF-2α (Xu *et al.*, 2011). Nevertheless HIF-1α alone is universally associated with the induction of pro-oncogenic features like tumor angiogenesis via VEGF (Jiang *et al.*, 1997). As an opposite example, in mammary carcinoma, HIF-1α was required for induction of a set of well-

characterized hypoxic genes in breast carcinoma cell lines, while HIF-2α inhibited the growth of the tumor cells (Blancher *et al*., 2000). The existence of the two isoforms and the diametrically opposed behavior raises the question whether they have in general control similar or even contrasting effects? Interestingly, in this study, FRET data manifestly revealed the homodimerization of HIF-1α/HIF-2α (Fig. 4-4), supported by co-immunoprecipitation experiment (Fig. 4-7). Still, no DNA-binding of the homodimeric complex (Fig. 4-11) and no considerable transcriptional activity (Fig. 4-15, lane 5) were observed. Most interestingly, it should be noted that HIF-2α overexpression inhibited HIF-1α to heterodimerize with ARNT by forming a DNA unbound complex HIF-1α/HIF-2α (Res. 4-3, Fig. 4-11). In support of this finding, the HIF-1α specific target gene carbonic anhydrase 9 mRNA expression level decreased considerably when cell were transfected to overexpress HIF-2α (Fig. 4-17). From these findings one may assume competition between ARNT – which was also abundant due to overexpression – and HIF-2α for HIF-1α: forming a HIF-1α/HIF-2α homodimer in a scenario of HIF-2α abundance could negatively regulate and thus fine-tune the expression of a HIF-1α/ARNT controlled gene such as CA9 (Fig. 5-3).

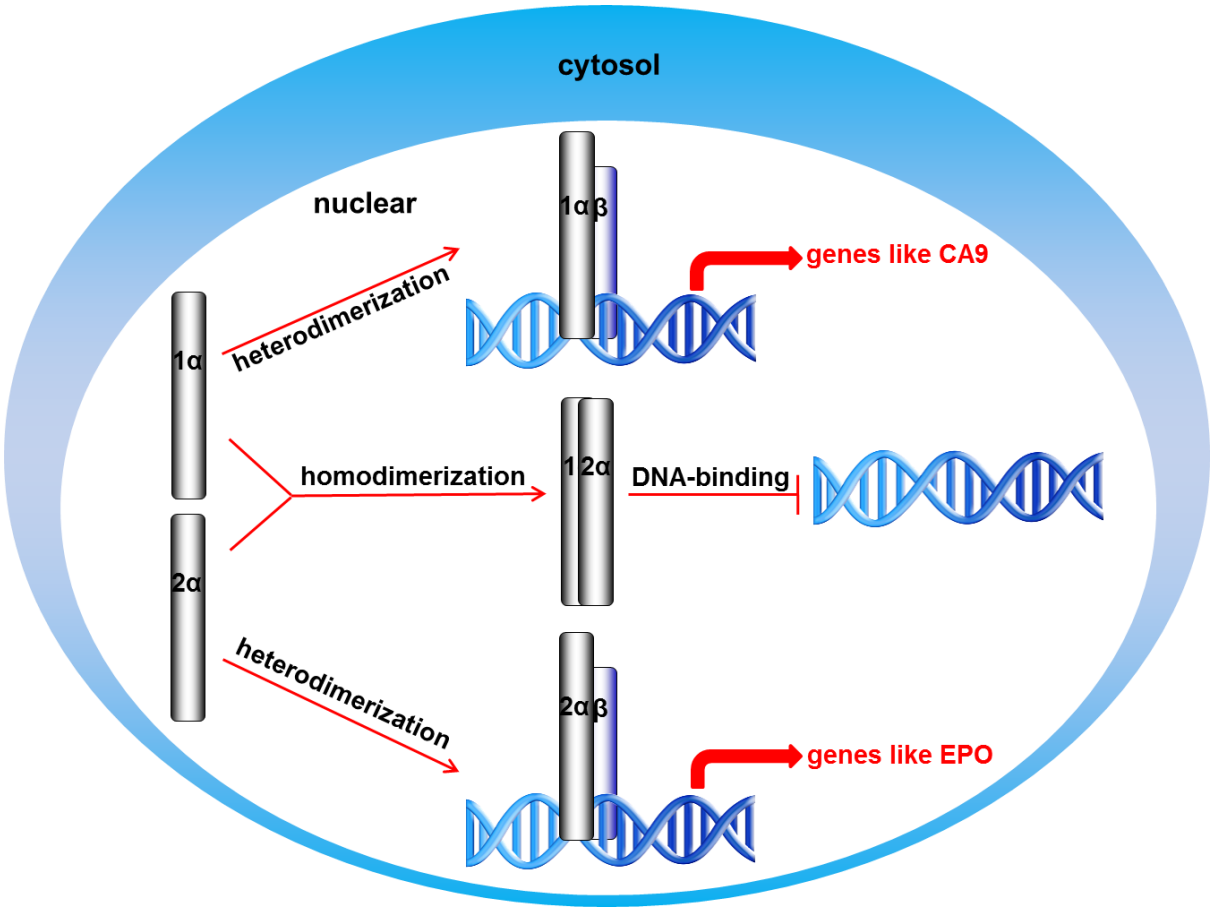

Fig. 5-3: Competition mechanism of HIF-1α and HIF-2α

In cell with both HIF-1α and HIF-2α, either subunit dimerized with ARNT can induce specific target genes or share common target genes. This was however prevented by forming a nonfunctional homodimer of HIF-1α/HIF-2α.

6. References

Berchner-Pfannschmidt, U., Frede, S., Wotzlaw, C., and Fandrey, J. (2008). Imaging of the hypoxia-inducible factor pathway: insights into oxygen sensing. *European Respiratory Journal, 32*(1), 210-217.

Berchner-Pfannschmidt, U., Tug, S., Trinidad, B., Oehme, F., Yamac, H., Wotzlaw, C., Flamme, I., and Fandrey, J. (2008). Nuclear oxygen sensing: induction of endogenous prolyl-hydroxylase 2 activity by hypoxia and nitric oxide. *Journal of Biological Chemistry, 283*(46), 31745-31753.

Berchner-Pfannschmidt, U., Yamac, H., Trinidad, B., and Fandrey, J. (2007). Nitric oxide modulates oxygen sensing by hypoxia-inducible factor 1-dependent induction of prolyl hydroxylase 2. *Journal of Biological Chemistry, 282*(3), 1788-1796.

Bernard, P., and Couturier, M. (1992). Cell killing by the F plasmid CcdB protein involves poisoning of DNA-topoisomerase II complexes. *Journal of Molecular Biology, 226*(3), 735-745.

Blancher, C., Moore, J. W., Talks, K. L., Houlbrook, S., and Harris, A. L. (2000). Relationship of hypoxia-inducible factor (HIF)-1α and HIF-2α expression to vascular endothelial growth factor induction and hypoxia survival in human breast cancer cell lines. *Cancer Research, 60*(24), 7106-7113.

Bruick, R. K., and McKnight, S. L. (2001). A conserved family of prolyl-4-hydroxylases that modify HIF. *Science Signaling, 294*(5545), 1337.

Card, P. B., Erbel, P. J., and Gardner, K. H. (2005). Structural basis of ARNT PAS-B dimerization: use of a common beta-sheet interface for hetero-and homodimerization. *Journal of Molecular Biology, 353*(3), 664-677.

Carretero-Paulet, L., Galstyan, A., Roig-Villanova, I., Martínez-García, J. F., Bilbao-Castro, J. R., and Robertson, D. L. (2010). Genome-wide classification and evolutionary analysis of the bHLH family of transcription factors in Arabidopsis, poplar, rice, moss, and algae. *Plant Physiology, 153*(3), 1398-1412.

Choi, S. M., and Park, H. (2009). The novel peptide F29 facilitates the DNA-binding ability of hypoxia-inducible factor-1alpha. *BMB Reports, 42*, 737-742.

Chowdhury, R., Hardy, A., and Schofield, C. J. (2008). The human oxygen sensing machinery and its manipulation. *Chemical Society Reviews, 37*(7), 1308-1319.

Covello, K. L., and Simon, M. C. (2004). HIFs, hypoxia, and vascular development. *Current Topics in Developmental Biology*, 62, 37-54.

Davis, R. L., Cheng, P.-F., Lassar, A. B., and Weintraub, H. (1990). The MyoD DNA binding domain contains a recognition code for muscle-specific gene activation. *Cell, 60*(5), 733-746.

Dioum, E. M., Rutter, J., Tuckerman, J. R., Gonzalez, G., Gilles-Gonzalez, M.-A., and McKnight, S. L. (2002). NPAS2: a gas-responsive transcription factor. *Science Signaling, 298*(5602), 2385.

Erbel, P. J., Card, P. B., Karakuzu, O., Bruick, R. K., and Gardner, K. H. (2003). Structural basis for PAS domain heterodimerization in the basic helix-loop-helix-PAS transcription factor hypoxia-inducible factor. *Proceedings of the National Academy of Sciences, 100*(26), 15504-15509.

Fandrey, J., and Gassmann, M. (2009). Oxygen sensing and the activation of the hypoxia inducible factor 1 (HIF-1)-invited article *Arterial Chemoreceptors* (pp. 197-206): Springer Publishers.

Fandrey, J., Gorr, T. A., and Gassmann, M. (2006). Regulating cellular oxygen sensing by hydroxylation. *Cardiovascular Research, 71*(4), 642-651.

Godlewski, J., Wang, S., and Wilson, T. G. (2006). Interaction of bHLH-PAS proteins involved in juvenile hormone reception in *Drosophila*. *Biochemical and Biophysical Research Communications, 342*(4), 1305-1311.

Gordan, J. D., and Simon, M. C. (2007). Hypoxia-inducible factors: central regulators of the tumor phenotype. *Current Opinion in Genetics and Development, 17*(1), 71-77.

Gu, Y.-Z., Hogenesch, J. B., and Bradfield, C. A. (2000). The PAS superfamily: sensors of environmental and developmental signals. *Annual Review of Pharmacology and Toxicology, 40*(1), 519-561.

Gu, Y.-Z., Moran, S., Hogenesch, J. B., Wartman, L., and Bradfield, C. A. (1998). Molecular characterization and chromosomal localization of a third alpha-class hypoxia inducible factor subunit, HIF3alpha. *Gene Expression, 7*(3), 205.

Holmquist-Mengelbier, L., Fredlund, E., Löfstedt, T., Noguera, R., Navarro, S., Nilsson, H., Pietras,.A., Vallon-Christersson,.J., Borg,.A., Gradin, K., and Pahlman, S. (2006). Recruitment of HIF-1α and HIF-2α to common target genes is differentially regulated in neuroblastoma: HIF-2α promotes an aggressive phenotype. *Cancer Cell, 10*(5), 413-423.

Hu, C.-J., Sataur, A., Wang, L., Chen, H., and Simon, M. C. (2007). The N-terminal transactivation domain confers target gene specificity of hypoxia-inducible factors HIF-1α and HIF-2α. *Molecular Biology Of the Cell, 18*(11), 4528-4542.

Hu, C.-J., Wang, L.-Y., Chodosh, L. A., Keith, B., and Simon, M. C. (2003). Differential roles of hypoxia-inducible factor 1α (HIF-1α) and HIF-2α in hypoxic gene regulation. *Molecular and Cellular Biology*, *23*(24), 9361-9374.

Hu, J., Stiehl, D. P., Setzer, C., Wichmann, D., Shinde, D. A., Rehrauer, H., Hradecky, P., Gassmann, M., and Gorr, T. A. (2011). Interaction of HIF and USF signaling pathways in human genes flanked by hypoxia-response elements and E-box palindromes. *Molecular Cancer Research*, *9*(11), 1520-1536.

Huang, L. E., and Bunn, H. F. (2003). Hypoxia-inducible factor and its biomedical relevance. *Journal of Biological Chemistry, 278*(22), 19575-19578.

Ivan, M., Kondo, K., Yang, H., Kim, W., Valiando, J., Ohh, M., Salic, A., Asara, J. M., Lane, W. S., and Kaelin Jr, W. G. (2001). HIFalpha targeted for VHL-mediated destruction by proline hydroxylation: implications for O_2 sensing. *Science Signaling*, *292*(5516), 464.

Jaakkola, P., Mole, D. R., Tian, Y.-M., Wilson, M. I., Gielbert, J., Gaskell, S. J., Von Kriegsheim, A., Hebestreit, H. F., Schofield, C. J., Maxwell, P. H., Pugh, C. W., and Ratcliffe, P. J. (2001). Targeting of HIF-alpha to the von Hippel-Lindau ubiquitylation complex by O2-regulated prolyl hydroxylation. *Science Signaling, 292*(5516), 468.

Jiang, B.-H., Agani, F., Passaniti, A., and Semenza, G. L. (1997). V-SRC induces expression of hypoxia-inducible factor 1 (HIF-1) and transcription of genes encoding vascular endothelial growth factor and enolase 1: involvement of HIF-1 in tumor progression. *Cancer Research, 57*(23), 5328-5335.

Jones, S. (2004). An overview of the basic helix-loop-helix proteins. *Genome Biology, 5*(6), 226.

Key, J., Scheuermann, T. H., Anderson, P. C., Daggett, V., and Gardner, K. H. (2009). Principles of ligand binding within a completely buried cavity in HIF2α PAS-B. *Journal of the American Chemical Society, 131*(48), 17647-17654.

Kondo, K., Kim, W. Y., Lechpammer, M., and Kaelin Jr, W. G. (2003). Inhibition of HIF2α is sufficient to suppress pVHL-defective tumor growth. *PLOS Biology, 1*(3), e83.

Lakowicz, J. (2006). Principles of Fluorescence Spectroscopy (3rd edit.) Springer. *New York, NY*.

Landy, A. (1989). Dynamic, structural, and regulatory aspects of lambda site-specific recombination. *Annual Review of Biochemistry, 58*(1), 913-941.

Lau, K., Tian, Y., Raval, R., Ratcliffe, P., and Pugh, C. (2007). Target gene selectivity of hypoxia-inducible factor-α in renal cancer cells is conveyed by post-DNA-binding mechanisms. *British journal of Cancer, 96*(8), 1284-1292.

Lee, K., Zhang, H., Qian, D. Z., Rey, S., Liu, J. O., and Semenza, G. L. (2009). Acriflavine inhibits HIF-1 dimerization, tumor growth, and vascularization. *Proceedings of the National Academy of Sciences, 106*(42), 17910-17915.

Letunic, I., Copley, R. R., Pils, B., Pinkert, S., Schultz, J., and Bork, P. (2006). SMART 5: domains in the context of genomes and networks. *Nucleic Acids Research, 34*(suppl 1), D257-D260.

Loboda, A., Jozkowicz, A., and Dulak, J. (2010). HIF-1 and HIF-2 transcription factors - similar but not identical. *Molecules and Cells, 29*(5), 435-442.

Michel, G., Minet, E., Ernest, I., Roland, I., Durant, F., Remacle, J., and Michiels, C. (2000). A model for the complex between the hypoxia-inducible factor-1 (HIF-1) and its consensus DNA sequence. *Journal of Biomolecular Structure and Dynamics, 18*(2), 169-179.

Murre, C., Bain, G., van Dijk, M. A., Engel, I., Furnari, B. A., Massari, M. E., Quong, M. W., Rivera, R. R., and Stuiver, M. H. (1994). Structure and function of helix-loop-helix proteins. *Biochimica et Biophysica Acta, N. Gene Structure and Expression, 1218*(2), 129-135.

Murre, C., McCaw, P. S., Vaessin, H., Caudy, M., Jan, L. Y., Jan, Y. N., Cabrera, C. V., Buskin, J. N., Hauschka, S. D., Lassar, A. B., Weintraub, H., and Baltimore, D. (1989). Interactions between heterologous helix-loop-helix proteins generate complexes that bind specifically to a common DNA sequence. *Cell, 58*(3), 537-544.

Möglich, A., Ayers, R. A., and Moffat, K. (2009). Structure and signaling mechanism of Per-ARNT-Sim domains. *Structure, 17*(10), 1282-1294.

Nytko, K. J., Maeda, N., Schläfli, P., Spielmann, P., Wenger, R. H., and Stiehl, D. P. (2011). Vitamin C is dispensable for oxygen sensing in vivo. *Blood, 117*(20), 5485-5493.

Patterson, G. H., Piston, D. W., and Barisas, B. G. (2000). Förster distances between green fluorescent protein pairs. *Analytical Biochemistry, 284*(2), 438.

Pingoud, A., and Jeltsch, A. (2001). Structure and function of type II restriction endonucleases. *Nucleic Acids Research, 29*(18), 3705-3727.

Ptashne, M., and Switch, A. G. (1992). Phage λ and Higher OrganismsCell Press and Blackwell Scientific Publications. *Cambridge, USA*.

Rankin, E., and Giaccia, A. (2008). The role of hypoxia-inducible factors in tumorigenesis. *Cell Death and Differentiation, 15*(4), 678-685.

Rankin, E. B., Biju, M. P., Liu, Q., Unger, T. L., Rha, J., Johnson, R. S., Simon, M. C., Keith, B., and Haase, V. H. (2007). Hypoxia-inducible factor-2 (HIF-2) regulates hepatic erythropoietin in vivo. *Journal of Clinical Investigation, 117*(4), 1068-1077.

Ratcliffe, P. J. (2007). HIF-1 and HIF-2: working alone or together in hypoxia? *Journal of Clinical Investigation, 117*(4), 862-865.

Raval, R. R., Lau, K. W., Tran, M. G., Sowter, H. M., Mandriota, S. J., Li, J.-L., Pugh, C. W., Maxwell, P. H., Harris, A. L., and Ratcliffe, P. J. (2005). Contrasting properties of hypoxia-inducible factor 1 (HIF-1) and HIF-2 in von Hippel-Lindau-associated renal cell carcinoma. *Molecular and Cellular Biology, 25*(13), 5675-5686.

Rolfs, A., Kvietikova, I., Gassmann, M., and Wenger, R. H. (1997). Oxygen-regulated transferrin expression is mediated by hypoxia-inducible factor-1. *Journal of Biological Chemistry, 272*(32), 20055-20062.

Sambrook, J., Fritsch, E., and Maniatis, T. (1989). Preparation and transformation of competent E. coli. *Molecular Cloning: A Laboratory Manual. Cold Spring Harbor Laboratory Press, Cold Spring Harbor*, 1.74-71.84.

Scheuermann, T. H., Tomchick, D. R., Machius, M., Guo, Y., Bruick, R. K., and Gardner, K. H. (2009). Artificial ligand binding within the HIF2α PAS-B domain of the HIF2 transcription factor. *Proceedings of the National Academy of Sciences, 106*(2), 450-455.

Schofield, C. J., and Ratcliffe, P. J. (2005). Signalling hypoxia by HIF hydroxylases. *Biochemical and Biophysical Research Communications, 338*(1), 617-626.

Semenza, G. L. (1996). Transcriptional regulation by hypoxia-inducible factor 1 molecular mechanisms of oxygen homeostasis. *Trends in Cardiovascular Medicine, 6*(5), 151-157.

Semenza, G. L. (1998). Hypoxia-inducible factor 1: master regulator of O_2 homeostasis. *Current Opinion in Genetics and Development, 8*(5), 588-594.

Semenza, G. L. (2001). HIF-1 and mechanisms of hypoxia sensing. *Current Opinion in Cell Biology, 13*(2), 167-171.

Semenza, G. L. (2001). HIF-1, O_2, and the 3 PHDs: How Animal Cells Signal Hypoxia to the Nucleus. *Cell, 107*(1), 1-3.

Skuli, N., Liu, L., Runge, A., Wang, T., Yuan, L., Patel, S., Iruela-Arispe, L., Simon, M. C., and Keith, B. (2009). Endothelial deletion of hypoxia-inducible factor-2α (HIF-2α) alters vascular function and tumor angiogenesis. *Blood, 114*(2), 469-477.

Sogawa, K., Nakano, R., Kobayashi, A., Kikuchi, Y., Ohe, N., Matsushita, N., and Fujii-Kuriyama, Y. (1995). Possible function of Ah receptor nuclear translocator (Arnt) homodimer in transcriptional regulation. *Proceedings of the National Academy of Sciences, 92*(6), 1936-1940.

Sowter, H. M., Raval, R., Moore, J., Ratcliffe, P. J., and Harris, A. L. (2003). Predominant role of hypoxia-inducible transcription factor (Hif)-1α versus Hif-2α in regulation of the transcriptional response to hypoxia. *Cancer Research, 63*(19), 6130-6134.

Szablowska-Gadomska, I., Zayat, V., and Buzanska, L. (2011). Influence of low oxygen tensions on expression of pluripotency genes in stem cells. *Acta Neurobiologiae Experimentalis, 71*(1), 86-93.

Van de Sluis, B., Mao, X., Zhai, Y., Groot, A. J., Vermeulen, J. F., van der Wall, E., van Diest, P J., Hofker, M. H., Wijmenga, C., Klomp, L. W., Cho, K. R., Fearon, E. R., Vooijs, M., and Burstein, E. (2010). COMMD1 disrupts HIF-1α/β dimerization and inhibits human tumor cell invasion. *The Journal of Clinical Investigation, 120*(6), 2119.

Vinson, C. (2005). A Rationally Designed Small Molecule That Inhibits the HIF-1alpha-ARNT Heterodimer from Binding to DNA in Vivo. *Science Signaling, 2005*(284), pe23.

Wang, G. L., Jiang, B.-H., Rue, E. A., and Semenza, G. L. (1995). Hypoxia-inducible factor 1 is a basic-helix-loop-helix-PAS heterodimer regulated by cellular O_2 tension. *Proceedings of the National Academy of Sciences, 92*(12), 5510-5514.

Wiesener, M. S., Jürgensen, J. S., Rosenberger, C., Scholze, C. K., Hörstrup, J. H., Warnecke, C., Mandriota, S., Bechmann, I., Frei, U. A., Pugh, C. W., Ratcliffe, P. J., Bachmann, S., Maxwell, P. H., and Eckardt, K.-U. (2003). Widespread hypoxia-inducible expression of HIF-2α in distinct cell populations of different organs. *The FASEB Journal, 17*(2), 271-273.

Wotzlaw, C., Otto, T., Berchner-Pfannschmidt, U., Metzen, E., Acker, H., and Fandrey, J. (2007). Optical analysis of the HIF-1 complex in living cells by FRET and FRAP. *The FASEB Journal, 21*(3), 700-707.

Xu, J., Wang, B., Xu, Y., Sun, L., Tian, W., Shukla, D., Barod, R., Grillari, J., Grillari-Voglauer, R., Maxwell, P. H., and Esteban, M. A. (2011). Epigenetic regulation of HIF-1α in renal cancer cells involves HIF-1α/2α binding to a reverse hypoxia-response element. *Oncogene, 31*(8), 1065-1072.

Yang, J., Zhang, L., Erbel, P. J., Gardner, K. H., Ding, K., Garcia, J. A., and Bruick, R. K. (2005). Functions of the Per/ARNT/Sim domains of the hypoxia-inducible factor. *Journal of Biological Chemistry, 280*(43), 36047-36054.

Yuan, G., Peng, Y.-J., Reddy, V. D., Makarenko, V. V., Nanduri, J., Khan, S. A., Garcia, J. A., Kumar, G. K., Semenza, G. L., and Prabhakar, N. R. (2013). Mutual antagonism between hypoxia-inducible factors 1α and 2α regulates oxygen sensing and cardio-respiratory homeostasis. *Proceedings of the National Academy of Sciences, 110*(19), E1788-E1796.

Zhu, J., Martinez-Yamout, M., Cardoso, R., Yan, J., Love, R. A., Grodsky, N., Brooun, A., and Dyson, H. J. (2012). Homodimerization of the PAS-B domains of hypoxia-inducible factors. *The Journal of Physical Chemistry B, 116*(23), 6960-6965.

7. Appendix

7.1 List of Abbreviations

Table 7-1 List of abbreviations

Abbreviations	*full name*
HIF	*hypoxia inducible factor*
FRET	*fluorescence resonance energy transfer*
bHLH	*basic-helix-loop-helix*
PAS	*Period/Arnt/Single-minded*
ARNT	*aryl hydrocarbon nuclear translocator*
ODD	*oxygen-dependent degradation*
TAD	*transactivation domain*
PHD	*prolyl hydroxylase-domain*
NLS	*nuclear localization sequence*
HBS	*HIF binding site*
HRE	*hypoxia response elements*
CA9	*carbonic anhydrase 9*
VEGF	*vascular endothelial growth factor*
ADM	*adrenomedullin*
EPO	*erythropoietin*
CBP	*cAMP response element binding protein*
FIH	*factor inhibiting HIF*
Bnip	*BCL2/adenovirus E1B interacting protein*
PGK	*phosphoglycerate kinase*
ROS	*reactive oxygen species*
EMSA	*Electro-Mobility-Shift assay*
EDTA	*ethylenediaminetetraacetic acid*

PBS	*phosphate buffered saline*
SDS	*sodium dodecyl sulfate*
TEMED	*tetramethylethylenediamine*
APS	*ammonium persulfate*
Tris	*tris(hydroxymethyl)aminomethane*
TBS-T	*tris-buffered saline-Tween*
GFP	*freen fluorescent protein*
CFP	*cyan fluorescent protein*
YFP	*yellow Fluorescent Protein*
DTT	*dithiothreitol*
GTC	*guanidium thiocyanate*
DEPC	*diethylpyrocarbonate*
RT	*reverse transcription*
PCR	*polymerase chain reaction*
qRT	*quantitative real time*
UV	*ultraviolet*
IHF	*Integration Host Factor*
Int	*integrase*
Xis	*excisionase*
Cm (R)	*chloramphenicol resistance*
PNK	*polynucleotide kinase*
TAE	*tris acetate-EDTA*
DMEM	*Eagle's minimal essential medium*
FCS	*fetal calf serum*

7.2 List of Figures

7.3 List of Tables

7.4 List of Cloned Plasmids

Table 7-2 List of cloned plasmids

pExp-YFP-ARNTΔbHLH	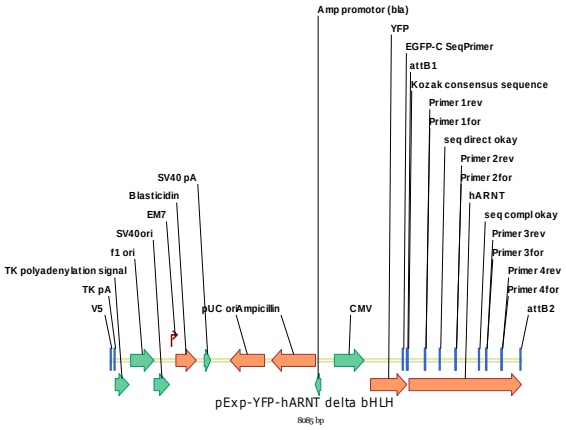
pExp-CFP-HIF-2αΔPASAB	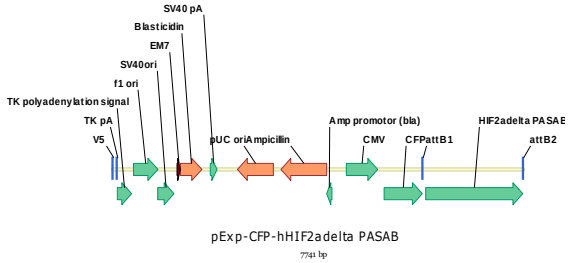
pExp-CFP-HIF-2αPASBm.	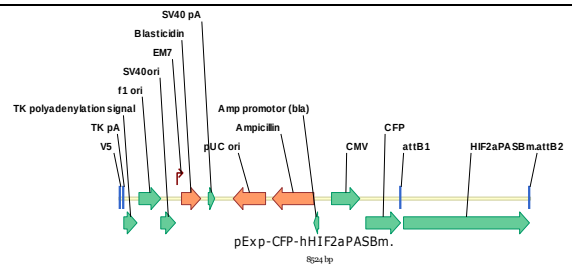

7.5 List of Publications

Publications:

1. Berchner-Pfannschmidt U, Tug S, **Hu J**, Reyes BD, Fandrey J, Kirsch M. (2010) *Role of N-acetyl-N-nitroso-tryptophan as nitric oxide donor in the modulation of HIF-1-dependent signaling.* Biol Chem. 391(5):533-40.
2. Wollenick K, **Hu J**, Kristiansen G, Schraml P, Rehrauer H, Berchner-Pfannschmidt U, Fandrey J, Wenger RH, Stiehl DP. (2012) *Synthetic transactivation screening reveals ETV4 as broad coactivator of hypoxia-inducible factor signaling.* Nucleic Acids Res. 40(5):1928-43.
3. Pientka FK, **Hu J**, Schindler SG, Brix B, Thiel A, Joehren O, Fandrey J, Berchner-Pfannschmidt U, Depping R. (2012) *Oxygen sensing by Prolyl-4-Hydroxylase PHD2 within the nuclear compartment and the influence of compartimentalisation on HIF-1 signalling.* J Cell Sci. 1;125(Pt 21):5168-76.
4. Submitting of first author paper

Congress Contribution (abstracts published):

1. **Hu J**, Konietzny R, Wotzlaw C, Bernardini A, Berchner-Pfannschmidt U, Fandrey J, (2010) *Interaction and mobiliy of hypoxia-inducible factors in living cells.* (poster) Annual Retreat of the DFG Graduate Training Program *Transcription, chromatin structure and DNA repair in development and differentiation* 1431, Essen Zollverein, Germany.
2. **Hu J**, Konietzny R, Wotzlaw C, Bernardini A, Berchner-Pfannschmidt U, Fandrey J, (2010) *Assembly of the transcription factor complex HIF for activation of the erythropoietin gene.* (poster) 9. Research Day of the Medical Faculty, University Hospital Essen, Germany.
3. **Hu J**, (2011) *Optical analysis of the basic-helix-loop-helix domain of hypoxia-inducible factors*. (presentation) Joint Annual Retreat of the Graduiertenkolleg 1431 and the BIOME 'Cell Biology and Genetics' Moduls, Dormagen-Zons, Germany.

4. **Hu J**, (2011) *Optical analysis of the basic-helix-loop-helix domain of hypoxia-inducible factors*. The Impact of Hypoxia on Cells, Mice and Men, Monte Verità - Ascona, Switzerland. (presentation, laureate of the best contribution for the oral presentation)
5. **Hu J**, Konietzny R, Wotzlaw C, Bernardini A, Berchner-Pfannschmidt U, Fandrey J, (2012) *Optical analysis of the hypoxia-inducible factors*. Annual Retreat of the DFG Graduate Training Program *Transcription, chromatin structure and DNA repair in development and differentiation* 1431, Techniker Haus Essen, Germany.
6. **Hu J**, (2013) *Optical analysis of the basic-helix-loop-helix and PAS domains of hypoxia-inducible factors 1 and 2*. Annual Retreat of the Graduiertenkolleg 1431, Ostbevern, Germany.

7.6 CV

The CV is not included in the online version due to the data protection.

7.7 Statement

Hereby I assure that, the present thesis titled with

„Quantitative Assessment of Dimer Formation by Hypoxia Inducible Transcription Factor Subunits HIF-1α and HIF-2α"

was written by myself and no other tools or sources out of the stated references was used. I assure that this thesis or thesis in similar form was not submitted in other university.

Essen, July 2013

SIGNATURE:_____

7.8 Acknowledgements

At first, I would like to thank Prof. Dr. J. Fandrey for giving me a good opportunity to do my Ph.D. work in his group and for lots of supports to my project, as well. Also, I would like to thank Prof. Dr. Carsten Schmuck to be the supervisor for my defense.

I really appreciate it that Dr. U. Berchner-Pfannschmidt was once the P.I. for my project and helped me a lot.

Thanks to Dr. R. Konietzny for establishing the Gateway system, to Dr A. Bernardini and Dr. C. Wotzlaw for the professional support in FRET study.

To Dr. T. A. Gorr and Mr. D. A. Shinde, your help to the EMSA experiments was greatly appreciated for my whole study.

I am grateful for the help of Prof. E. Metzen and Dr. U. Brockmeier in the aspect of molecular cloning and cell line establishing.

Indeed, I would like to express my gratitude to the whole group members in Institute of Physiology. Without you, I could not finish my work successfully.

Finally, thanks to my parents for the financial support and I really appreciate for your understanding.

Also, thanks to the DFG (Deutsche Forschungsgemeinschaft) for the three years of funding.